LATTICE DISTORTION AND CHEMICAL ORDERING IN A COBALT-PLATINUM ALLOY

A Thesis

Submitted to

the Faculty of Graduate Studies

University of Manitoba

In Partial Fulfillment

of the Requirements for the Degree

Master of Science

by

Paul Jacob Tivin

Winnipeg, Canada

July 1971

TABLE OF CONTENTS

LIST OF FIGURES

ACKNOWLEDGEMENTS

I would like to thank my supervisor, Dr. Paul Gaunt, for his assistance during the course of this work.

I would also like to thank the members of the electronics and machine shops for their invaluable aid.

DEDICATION

To my parents for their patience and understanding.

ABSTRACT

The long-range order parameter of CoPt has been measured by X-ray diffraction techniques. The experimental results are compared with theoretical results derived on the basis of a lattice distortion dependent energy theory. The theoretical and experimental results are in fair agreement. The theory is compared with the experimental results for CuZn, but the best agreement with the experimental results is shown to be by the compressible Ising model lattice.

I. Introduction

A. Order-Disorder Phenomena

Among the many interesting properties exhibited by alloys is the phenomenon of the order-disorder transformation. Qualitatively, what is meant by the term "order" is the excess probability over randomness that there exist correlations in the manner of occupation of lattice sites by the atoms that constitute the alloy. Similarly, the term "disorder" will mean that the probability of correlations in the occupation of the lattice sites by the atoms of the alloy is simply random. Quantitative definitions of these terms will be taken up later.

We can see that one or more parameters are needed to distinguish between the states of order and disorder. The manner of definition of such parameters is, of course, not unique but the conventional ones are a long-range order parameter, S, introduced by Bragg and Williams, and a short-range order parameter, σ, introduced by Bethe.[1]

Figures 1 and 2 help to illustrate these two parameters. In Figure 1 we see that all the lattice sites are occupied in a manner such that the nearest neighbors of either type of atom are all atoms of the opposite type. In Figure 2 some of the lattice sites have for nearest neighbors equal numbers of the two types of atoms while other lattice sites have for nearest neighbors predominantly atoms of the opposite type. If we divide these lattices

into two sub-lattices and require that atoms represented by an open circle occupy only one sub-lattice and atoms represented by filled circles occupy only the other sub-lattice, then in Figure 1 we may say that long-range order exists while in Figure 2 only short-range order exists.

Such two-dimensional representations can easily be extended to three dimensions, for which a typical example is the ordered alloy CuZn or β-brass. In Figure 3 is shown the unit cell of CuZn in the ordered phase. One type of atom, say the Cu, occupies the cube corners while the other atom, Zn, occupies the cube center. In this phase the nearest neighbors of the Zn atoms are 8 Cu atoms and vice versa. In the disordered phase of this alloy four of the 8 nearest neighbors of an atom become atoms of the same type.

As an aside, we may note that the idea of order-disorder phenomena is exactly analogous to the ferromagnetic-paramagnetic phenomena.[2] More generally, ferromagnetic and order-disorder behavior are manifestations of many-body co-operative behavior. The co-existence of these two phenomena has long been noticed in various alloys. On the other hand, the theory which includes both ferromagnetism and ordering at the same time encounters a mathematical difficulty of finding the equilibrium conditions because of the complexity of the fundamental equations and the lack of knowledge about the elementary interactions.[3]

Furthermore, the effect of ordering on many other physical properties is quite important. For example, we may

expect that the energy associated with an ordered arrangement of atoms in an alloy is relatively small compared with the energy of a disordered arrangement. Thus, this energy associated with increasing disorder will contribute to the specific heat of the alloy in such a manner that the specific heat of the alloy will be in excess of the value expected from calculations based on lattice vibration effects only. This excess specific heat is known as "the configurational specific heat". The variation of the specific heat of an alloy with temperature approaches a sharp maximum as the temperature increases due to the large energy changes caused by increasing degree of disorder. This maximum reaches its peak at the critical temperature for the order-disorder transition. Above the critical temperature the long-range order has disappeared and the only further changes in the ordering of the structure with increasing temperature are relatively small changes in the remaining short-range order, and consequently it is expected that the excess specific heat above the critical temperature is small. These ideas are exhibited in Figure 4.[4]

Another property of alloys which changes with the degree of order is the electrical resistivity. One would expect from quantum mechanical considerations that the electrical resistivity of a perfect crystal would be zero. However, the resistivity arises from collisions between the conduction electrons and lattice phonons, impurities, or departures from lattice periodicity.[5] While the resistivity

increases normally with temperature, the rate of increase of resistivity is anomalously large until the critical temperature for the order-disorder transition is reached. Beyond the critical temperature this anomalous rate of increase of resistivity disappears. Thus the resistivity shows no discontinuity but the rate of increase shows a sharp discontinuity. Qualitatively this result can be understood by considering the imperfections of the superlattice. These cause irregularities in the generally periodic electric field in which the electrons move and are very effective in scattering the conduction electrons. This result is effectively illustrated in Figure 5.[6]

Of other electrical properties that have been found to depend sensitively upon the state of order, the Hall coefficient is of particular interest in that it gives information about the nature of the charge carriers, or, alternatively, about the band structure of the material.[7] A change of sign in the Hall coefficient will indicate that the charge carrier has changed its sign due to a change in the band structure.

It has already been mentioned that ferromagnetic properties can be influenced by the degree of order in an alloy. As an example, we can consider the effect of ordering on the saturation moment of Ni_3Mn. Ordering may split the electron band and, hence, may alter the density of states versus energy curve. The result is shown in Figure 6 where C_{el}/T is plotted against T^2 where C_{el} is the electronic specific

heat. The slope of the curve, γ, is directly proportional to the density of states at the Fermi surface.[8] The values of γ are 11.7 and 22.4 x 10^{-4} for the ordered and disordered Ni_3Mn, respectively. Since the ordered alloy is ferromagnetic, it is probable that the half band of one spin is full or nearly full and, hence, only electrons of the other spin can contribute to the electronic specific heat. A schematic representation of the density of states is shown in Figure 7 and illustrates a qualitative picture of the d band in ordered and disordered Ni_3Mn.[9] Since the degree of ferromagnetism of Ni_3Mn depends upon the state of order, a maximum in the magnetization should be expected for the ordered alloy at the Ni_3Mn composition. Such a result is shown in Figure 8.

As a final, note it should be expected that the mechanical properties, such as Young's modulus and the shear constants, will be related to the degree of order in an alloy. Such an effect is shown in Figure 9 for the alloy Cu_3Au. The curve shows the difference between the extrapolated values of $C_{11} - C_{12}$ and C_{44} for complete order and complete disorder and the measured values of these two quantities.[10]

B. The Alloy CoPt

Below the solidus curve Cobalt and Platinum form a continuous series of solid solutions, although transformations based on the alloys containing 25 and 50 atomic per cent Cobalt occur at lower temperatures.

The phase diagram for the system Cobalt-Platinum is presented in Figure 10.[11] We note that there is an asymmetry of the ordering range about the 50 atomic per cent composition in that there is an ordered alloy of composition Pt_3Co but none of composition $PtCo_3$. Such an asymmetry is not unusual, having been found in such systems as CuPt, CuPd, and CuAu.[12]

From the phase diagram we see that the alloy of composition CoPt, when ordered, has the face-centered tetragonal structure, and, when disordered, has the face-centered cubic structure. Figure 11 shows the face-centered cubic structure while Figure 12 shows the face-centered tetragonal structure.

Direct evidence for ordering was first provided by Gebhardt and Koster[13] who showed that the face-centered cubic structure of alloys containing approximately equal proportions of the two types of atoms transformed into one having tetragonal symmetry at temperatures below 825 °C. Hultgren and Jaffe showed that the ordered tetragonal phase was stable up to 800 °C if sufficiently prolonged heat treatments were employed.[14] The stability of the ordered face-centered tetragonal phase at all temperatures up to 825 °C was finally established by Newkirk et al.[15]

The order ing reaction is relatively sluggish and requires several hundred hours of heat treatment, of course depending upon the temperature of the heat treatment, to attain equilibrium in the duplex field. The Cobalt and

Platinum atoms arrange themselves during the ordering on alternate planes, thus forming discrete particles having tetragonal symmetry. Growth occurs in such a manner that the <100> directions of the ordered particles are parallel with the corresponding axes of the parent lattice. In the early stages of the process considerable stresses are caused by platelets of the tetragonal phase which lie on and are coherent with the (110) planes of the cubic lattice. These stresses are accompanied by a self deformation process which gives rise to twinning and by recrystallization which predominates at the lower ageing temperatures. In the duplex regions the ordered phase assumes a Widmanstatten structure, that is, a plate-like or lamellar structure aligned with the (100) planes of the disordered lattice.[16]

The thermodynamic properties of the Co-Pt system have been investigated by Oriani.[17] It was observed that the Co-Pt system showed deviations from the predictions of the nearest-neighbor interaction theories of order-disorder in that the observed heat of solution is positive not negative, the entropy of solution is much larger than the ideal value, and though the deviations from Raoult's Law for the Cobalt are negative throughout, the deviations for Platinum are positive for much of the composition range. Oriani accounts for these deviations qualitatively by suggesting the existence of a vibrational-entropy contribution to the entropy of solution which may include as an important factor a volume change, and a strain-energy contribution to the heat of solution.

An interesting anomaly in the electrical properties of CoPt is the fact that at the equilibrium temperature the resistance of the ordered phase is higher than that of the disordered phase. This is contrary to the classical theories of ordering. At temperatures much below the critical temperature, though, the resistance decreases upon ordering in the conventional manner.[18]

The most important properties, from the practical point of view, of the Co-Pt system are its magnetic properties. The outstanding permanent magnet properties of the 50 atomic per cent alloy were first reported by Jellinghaus[19] who found that a coercive force of 4000 oersteds could be developed by quenching and ageing cast material of this composition. By suitable heat treatments coercive forces of the order of 4000 oersteds can be obtained in conjunction with maximum energy products of 9×10^6 gauss-oersted. These values were the highest known for any alloy until the development of $SmCo_5$ alloys. Although the maximum energy products and coercive forces are developed in alloys close to the equi-atomic composition these paremeters are so powerfully affected by slight difference of heat treatment that the effects of composition variations are not easily discerned. The optimum magnetic characteristics are attained by the development of a partly ordered structure having the two phases present in similar proportions. The diffuse

diffraction lines characteristic of material in this condition have been interpreted as evidence for a coherent bond between the ordered phase and its matrix. Several types of heat treatment are employed to develope the desired magnetic characteristics in Cobalt-Platinum alloys. An essential feature of one widely used process is the strictly controlled cooling rate from 1000°C to 200°C at 1 to 10° per second which precedes an ageing treatment at 600°C. Another process proceeds by quenching from the disordering temperature to 500 to 750°C, the alloy being maintained at the final temperature for periods up to five hours. To magnetize the alloy after such heat treatments field strengths of the order of 20,000 oersteds are required. In Figures 13 and 14 are illustrated the test characteristics of a specimen which was annealed at 1000°C for two hours, then quenched to 660°C and held at that temperature for forty-five minutes. It has been suggested that the permanent magnet properties of Cobalt-Platinum are explicable on the basis of single domain particle theory, but Craik and Nunez[20] have shown that only a small proportion of the ordered region consists of single domains. The high coercive force of Cobalt-Platinum is now generally attributed to the large localized strains induced by the ordering process, and the effectiveness of the various heat treatments employed is probably due entirely to the high internal stresses which they generate. Woolley and Bates[21] suggest that the optimum magnetic condition corresponds to the incipent stage when the nuclei

of the ordered phase remain coherent with the disordered matrix, thus causing large localized strains. At room temperature the (110) plane of the disordered phase is 0.18 per cent smaller in area than the (101) plane of the ordered phase with which it is coherent. This difference in area diminishes as the temperature increases, thus accounting for the rapid decrease in coercive force which occurs upon heating.

II. Theories of Order-Disorder

In the preceding chapter the quantities S and σ have been introduced which allow two particular properties, the long-range and short-range order respectively, of a given configuration of an alloy to be specified in a precise manner. Now we wish to develope quantitative treatments of the equilibrium values of these quantities, and related quantities of interest, as functions of the temperature and composition of the alloy. The problem then is to write an approximate partition function which can be handled without undue mathematical rigor but which is sufficiently close to a rigorously correct partition function to give predictions of interest and value.

Quite generally the complete partition function for the crystal may be written

$$Z = \sum_{\alpha} \exp(-\beta E_{\alpha}) \qquad (1)$$

where $\beta = 1/kT$ and E_{α} is the energy of the state α obtained by solution of the complete Schrodinger equation for the crystal and the summation is taken over all states of the crystal. If we assume that the complete Schrodinger equation is separable, then the complete Hamiltonian and wave function may be written as

$$H = H_1 + H_i + H_e$$
$$\psi = \psi_1 \psi_i \psi_e \qquad (2)$$

where H_1 and ψ_1 are functions of variables specifying a crystal of structureless particles; H_i and ψ_i are functions of variables specifying the internal structure of the

actual ions of the crystal; and H_e and ψ_e are functions of variables specifying the remaining electrons considered as moving in the potenial field of the ions. The assumption of separability implies that each eigenvalue of the Schrodinger equation may be written

$$E = E_e + E_1 + E_i \qquad (3)$$

where the E_1, E_i, E_e are solutions of the separate equations $H_1\psi_1 = E_1\psi_1$ etc., and are generally functions of the configurations of the crystal. The partition function, (1), becomes

$$Z = \sum_c \left(\sum_1 e^{-\beta E_1} \sum_e e^{-\beta E_e} \sum_i e^{-\beta E_i} \right) \qquad (4)$$

where the summations involving 1, e, and i, are made over all eigenvalues E_1, E_e, and E_i appropriate to a given configuration of the crystal and the ( ) is summed over all possible distinguishable configurations, labelled "c", of the crystal. Now H_1 and E_1 are written as

$$\begin{aligned} H &= H_{kin} + V_{config} + V_{disp} = H_1' + V(c) \\ E &= E_1' + V(c) \end{aligned} \qquad (5)$$

where H_{kin} is the kinetic energy part of the Hamiltonian due to the ions, $V_{config} = V(c)$ is the part of the potenial energy due to the ions being in their equilibrium position in the configuration labelled "c", and V_{disp} is the contribution to the potenial energy due to the displacement of the ions from their equilibrium position. It is now assumed that the dependence of H_1 and H_e and consequently E_1 and E_e on the configuration parameters may be ignored; that is, they are the same for all configurations. Then (4) may be

written

$$\mathcal{Z} = \left(\sum_{1} e^{-\beta E_1'} \sum_{e} e^{-\beta E_e} \sum_{i} e^{-\beta E_i} \right) \sum_{c} e^{-\beta V(c)} \qquad (6)$$

For the difference in equilibrium thermodynamic quantities calculated (a) for a crystal in which configurational effects are ignored, and (b) for the same crystal with configurational effects included; it is sufficient to consider only the last term in (6) and write

$$\mathcal{Z} = \sum_{c} e^{-\beta V(c)} \qquad (7)$$

since the other factors will cancel in the calculations. It should be noted that the assumptions made cannot be rigorously true; there are in general interactions between the various components of a crystal which make it impossible to specify the state of one component with out reference to the state of other components.

Every distinguishable configuration of the alloy contributes a term to the sum in (7). Labelling these terms by "r" which represents a set of order parameters appropriate to the configuration from which the term arises, then (7) becomes

$$\mathcal{Z} = \sum_{r} z(r) \qquad (8)$$

where z(r) denotes the sum of all terms of a given r. Now in the determination of the equilibrium properties from Z it can be shown that we may replace lnZ by lnz(r*) where r* is the value of r for which z(r) has its largest value. Then the problem is to find z(r) for arbitrary r and then to find the value of r* which maximizes z(r). Now by

definition

$$z(r) = \sum_j e^{-\beta W_j} \qquad (9)$$

where W_j denotes the configurational energy V(c) for a configuration state "j" with the set of order parameters r and the summation is over all configurational states j appropriate to the set of order parameters r. Thus it becomes necessary to consider in detail the configuration energy W_j. The assumption to be made here is that the configuration energy may be written as a sum of interaction energies between pairs of atoms and that, in particular, interactions between all but nearest neighbor pairs of atoms may be neglected. This is a quite crude approximation to the actual configuration energy however. Now for a binary alloy composed of atoms of types A and B, the interaction energy of nearest neighbor AA, AB, and BB pairs in the AB alloy will, in general, be different and the number of such pairs will vary over the set of configurations of different r. In any specified configuration j our assumption allows the configurational energy to be written as

$$W_j = -2/h \left(n_{AA} J_{AA} + n_{BB} J_{BB} + n_{AB} J_{AB} \right) \qquad (10)$$

where h is the number of nearest neighbor sites of a given site in the lattice; $-2J_{AA}/h$, $-2J_{BB}/h$, and $-2J_{AB}/h$ are the energies of interaction of AA, BB, and AB pairs of nearest neighbors respectively; and n_{AA}, n_{BB}, and n_{AB} are the numbers of such pairs in the jth configuration.

Having now obtained a specification of W_j it is now necessary to consider the problem of the definition of the

degree of order in an alloy. For this let us consider in a given alloy that there are N lattice points occupied by N atoms of two kinds all of which take part in the ordering process. Other atoms, if present, of the same or different kinds, on other lattice points which take no part in the ordering may be ignored. It is to be emphasized that we are concerned with the given number of lattice sites and not necessarily the number of atoms since they are of two kinds and may be present in varying proportions.

We consider the lattice sites divided into two sub-lattices; and, in particular, we consider the two sub-lattices to be equivalent, that is each a site has only b nearest neighbors and vice versa. An example of such a lattice system is the body-centered cubic structure of CuZn depicted in Figure 3. Then there are $\frac{1}{2}N$ sites of type a and $\frac{1}{2}N$ of type b; each a site has h b sites as its nearest neighbors and each b site has h a sites for nearest neighbors.

For simplicity we first consider the case of equal numbers, $\frac{1}{2}N$, of each kind of atom A and B. Without loss of generality we can assume that at least half of the A atoms are on a sites. If we then denote the number of A atoms on a sites by $\frac{1}{2}(1+S)N/2$, the parameter S satisfies the inequality $0 \leq S \leq 1$. Since all A atoms not on a sites are on b sites, and all sites not occupied by A atoms are occupied by B atoms, the distribution of atoms is given by Table I. When S=1 all the A atoms are on a sites and all the B atoms

are on b sites; this is the state of perfect order. When S=0 there are as many A atoms on a sites as on b sites, similarly for the B atoms; this is the state of complete disorder where the distinction between a and b sites has disappeared. Intermediate values of S correspond to intermediate degrees of order and S is therefore a measure of the degree of order.

Now let us consider the case of unequal numbers of A and B atoms. There are a total of N atoms in the alloy of which N_A are A atoms and N_B are B atoms ($N_A+N_B=N$). If we write the number of A atoms as n_AN and B atoms as n_BN then we have

$$n_A + n_B = 1 \qquad (11)$$

and n_A is the fraction of A atoms in the alloy and n_B the fraction of B atoms in the alloy. If the number of A atoms on a sites is given by $n_A(1+S)N/2$, then the distribution of A and B atoms on the two types of sites is that given in Table II.

We are now in a position to consider the various approximations used to evaluate (8).

A. The Zeroth Approximation: Bragg and Williams[22]

In this approximation the set of order parameters r labelling the groups of terms in (8) is just taken to be the single long-range order parameter S; and the approximation consists in replacing the true value of W_j in (9) for each configuration j of given S by a simple average, $\bar{W}(s)$, over all configurations of the given S. Then (10) becomes

where $\bar{n}_{AA}$, $\bar{n}_{BB}$, and $\bar{n}_{AB}$ are the simple unweighted averages of n_{AA}, n_{BB}, and n_{AB} over all configurations j of given S. For a binary alloy for which the ordering may be described in terms of two equivalent sub-lattices, the distribution of A atoms on a sites is given by Table II; that is, the average number of A atoms on a sites is $n_A(1+S)N/2$ and each of these sites has h nearest neighbor b sites for which the average fractional occupation by A atoms is $n_A(1-S)$. Hence

$$\bar{n}_{AA} = h\,N/2\; n_A^2\,(1-S^2) \qquad (13)$$

In a similar manner we have

$$\bar{n}_{BB} = h\,N/2\,(n_B^2 - n_A^2 S^2)$$
$$\bar{n}_{AB} = h\,N/2\,(2n_A n_B + 2n_A^2 S^2) \qquad (14)$$

Now substituting (13) and (14) into (12) we have

$$\bar{W}(S) = -N\,(n_A^2 J_{AA} + 2n_A n_B J_{AB} + n_B^2 J_{BB}) + N n_A^2 S^2 (J_{AA} + J_{BB} - 2J_{AB}) \qquad (15)$$

If we write $J=2J_{AB}-J_{BB}-J_{AA}$, then

$$\bar{W}(S) = W(0) - N n_A^2 S^2 J \qquad (16)$$

where $W(0)=-N(n_A{}^2J_{AA}+2n_An_BJ_{AB}+n_B{}^2J_{BB})$. We note that for $J>0$ the configuration energy decreases for increasing S; this is the effect tending to produce long-range order but is counterbalanced by the decrease in the number of available configurations of given S as S increases.

From (9) we now have

$$\mathcal{G}(S) = g(S)\,\exp\left[-\frac{W(0) + N n_A^2 S^2 J}{kT}\right] \qquad (17)$$

where g(S) is the number of distinguishable configurations

of given S, or g(S) is the number of distinguishable ways of arranging the $n_A N$ A atoms and $n_B N$ B atoms on the sites of the crystal lattice so that there are $n_A(1+S)N/2$ A atoms on a sites and $n_A(1-S)N/2$ A atoms on b sites. This number is

$$g(S) = \frac{(N/2)!}{(n_A N/2\,(1+S))!\,[(n_B - n_A S)\frac{N}{2}]!} \times \frac{(N/2)!}{[n_A(1-S)N/2]!\,[(n_B+n_A S)N/2]!} \qquad (18)$$

Substituting (18) into (17) gives us an explicit expression for z(S). Now z(S) is maximized with respect to S by considering

$$\frac{\partial}{\partial S} \ln z(S) = 0 \qquad (19)$$

which can be evaluated with the help of Stirling's approximation. The result is

$$\ln\left[\frac{(n_A + n_A S)(n_B + n_A S)}{(n_A - n_A S)(n_B - n_A S)}\right] = \frac{4 n_A J}{kT} S \qquad (20)$$

Now the complete partition function as given by (8) may be taken equal to the single term z(S) with S obtained from (20). From the usual formula of statistical mechanics we obtain for the Helmholtz free energy

$$\begin{aligned} F(S) &= -kT \ln Z \\ &= NkT/2\,[(n_A + n_A S)\ln(n_A + n_A S) + (n_B - n_A S)\times \\ &\quad \ln(n_B - n_A S) + (n_A - n_A S)\ln(n_A - n_A S) + \\ &\quad (n_B + n_A S)\ln(n_B + n_A S)] + W(0) - N n_A^2 S^2 J \end{aligned} \qquad (21)$$

We now consider the form taken by the solutions to (20): (a) for the case $J<0$ then for all values of kT/J S=0 is the only solution and corresponds to a minimum in F(S) which means that there is no long-range order and therefore the alloy forms what is known as a regular solution which may be single phase or two phase depending on the

value of J/kT; (b) for J>0 and for high enough values of temperature S=0 is still the only solution to (20) and again corresponds to a minimum in F(S) with the alloy behaving as a regular solution. For sufficiently low values of temperature, S=0 is no longer the only root of (20) however; there is another root $0 \leq S \leq 1$ which corresponds to a minimum in F(S), the root S=0 now corresponding to a maximum. These effects are illustrated in Figure 15 in which F(S) is plotted as a function of S for differing values of J/kT for the particular case $n_A = n_B = \frac{1}{2}$. From Figure 15 it is seen that the equilibrium value of S decreases as the temperature increases, becoming zero at some temperature $T = T_c$ and remaining zero for all higher temperatures. The temperature T_c is called the critical temperature of the order-disorder transition and is the temperature at which (20) has two coincident roots at S=0, or alternatively the curve of F(S) against S has a point of inflection at S=0. The condition for determining T_c is therefore

$$\left(\frac{\partial F}{\partial S}\right)_{S=0} = 0 \qquad (22)$$

from which (21) gives

$$kT_c = 2 n_A n_B J \qquad (23)$$

It is seen from (23) that the values of T_c are the same for two alloys with compositions symmetrical with respect to the 50-50 alloy($n_A = n_B = \frac{1}{2}$), the variation of T_c with n_A being parabolic with a maximum value

$$kT_c = J/2 \qquad (24)$$

for the 50-50 alloy.

We may eliminate the parameter J now by means of (24), for the 50-50 alloy, and (20) becomes

$$\ln\left(\frac{1+S}{1-S}\right) = 2\,T_c/T\,S$$

or

$$\frac{T}{T_c} = \frac{S}{\tanh^{-1} S} \qquad (25)$$

Finally the configurational specific heat may be obtained from

$$\frac{C}{Nk} = \frac{1}{Nk}\,\frac{dE}{dS}\,\frac{dS}{dT}$$

which gives the result

$$\frac{C}{Nk} = \left(\frac{T_c}{T}\right)^2 S\left[\frac{1}{1-S^2} - \frac{T_c}{T}\right]^{-1} \qquad (26)$$

B. The First Approximation: The Quasi-chemical Method

The approximation involved in (10), (13), and (14) is very rough in that it completely avoids any effects of the details of the different configurations of given long-range order S; such neglect is unavoidable so long as the treatment is framed in terms of the single long-range order parameter, S, alone. For example, two configurations, each with the same value of $S \ll 1$, may differ widely in their degree of local ordering; one being very well ordered locally, the other being almost completely disordered. Such configurations would have very different configuration energies associated with them. The approximation of (10), (13), and (14) assume that such effects may be ignored; or more precisely, that the only configurations which make an effective contribution to the partition function are those for which the arrangement of A and B atoms on the sub-lattice is

effectively random provided that the given value of S is preserved.

In the present section a treatment will be described which involves two order parameters rather than the single parameter S of the previous section and which will allow these defects to be, in part, removed.

We shall denote by p the conditional probability that if an a site is occupied by an A atom then the nearest neighbor b site is also occupied by an A atom; and we shall let f_a and f_b be the fractional occupation numbers of a and b sites by A atoms ($f_a+f_b=2n_A$). As before there are a total of N lattice sites each of which has h nearest neighbors. Then Table III gives the number of pairs of neighboring sites in the lattice occupied in the four possible ways.

Now we may write an expression for the configuration energy, given by (10), in the nearest neighbor approximation. We have

$$W(f_a, p) = -2Nn_A J_{AB} - N(n_B - n_A) J_{BB} + Nf_a p J \qquad (27)$$

Now the partition function may be written

$$Z = \sum_{f_a, p} z(f_a, p) \qquad (28)$$

where the sum is over all possible values of f_a and p, and $z(f_a, p)$ is the contribution to the partition function from configurations of given f_a and p. As we have seen, however, all configurations of given f_a and p have the same configuration energy and so $z(f_a, p)$ may be written

$$z(f_a, p) = g(f_a, p) \exp\left[-W(f_a, p)/kT \right] \qquad (29)$$

where $g(f_a, p)$ is the number of configurations of given f_a

and p. The problem now is to evaluate $g(f_a,p)$ and then maximize $z(f_a,p)$ with respect to f_a and p. Unlike the zeroth approximation, however, we now have no simple value of g. There are in all Nh/2 nearest neighbor pairs in the lattice; the approximation of the present method is that, for given f_a, $g(f_a,p)$ is proportional to the total number of ways in which the Nh/2 possible pairs may be divided into the four groups of Table III, which becomes (30)

$$g(f_a,p) = h(f_a) \frac{(Nh/2)!}{(Nhf_a(1-p)/2)!\,(Nhf_ap/2)!\,(Nh(f_b-f_ap)/2)!\,(Nh(1-2n_A+f_ap)/2)!}$$

It must be noted that this formula cannot be exact; and, in point of fact, it is inexact in a manner similar to that in which (12) in the previous approximation was inexact.

Equation (30) is equivalent to assuming that the different pairs of neighbors may be treated as quite independent quantities. This cannot be true since, as soon as the nature of occupation of pairs of sites is fixed, the possible manners of occupation of other pairs which share a site with the first pair are limited. It is not easy to see, a priori, how bad this approximation is; although it would certainly be expected to be better than that involved in the previous treatment since, in a sense, the approximation is more limited in that it involves the order parameter p only. The number of configurations of given f_a alone will be given exactly since the function $h(f_a)$ is to be determined so that

$$\sum_p g(f_a,p) = g(f_a) = \frac{(N/2)!}{(Nf_a/2)!\,(N(1-f_a)/2)!} \frac{(N/2)!}{(Nf_a/2)!\,(N(1-f_b)/2)!} \quad (31)$$

The function $h(f_a)$ is determined quite simple. By a now

familiar argument we can show that we can replace

$$\sum_{p} g(f_a, p)$$

by $g(f_a, p^*)$ where p^* is the value of p which maximizes $g(f_a, p)$, thus

$$g(f_a, p^*) = \frac{(N/2)!}{(Nf_a/2)!\,(N(1-f_a)/2)!}\;\frac{(N/2)!}{(Nf_b/2)!\,(N(1-f_b)/2)!} \qquad (32)$$

But $g(f_a, p^*)$ is a particular solution to (30); thus by combining (30) and (32) we may determine $h(f_a)$ as a function of f_a and p^*. Now p^* is the value of p which corresponds to a completely random arrangement for the given f_a, that is $p^*=f_b$. Thus (30) becomes

$$g(f_a, p) = \frac{(N/2)!}{(Nf_a/2)!\,(N(1-f_a)/2)!}\;\frac{(N/2)!}{(Nf_b/2)!\,(N(1-f_b)/2)!}\;\frac{(Nhf_af_b/2)!}{(Nhf_ap/2)!}\times$$
$$\frac{(Nhf_a(1-f_b)/2)!}{(Nhf_a(1-p)/2)!}\;\frac{(Nhf_b(1-f_a)/2)!}{(Nh(f_b-f_ap)/2)!}\;\frac{(Nh(1-2n_A+f_af_b)/2)!}{(Nh(1-2n_A+f_ap)/2)!} \qquad (33)$$

By substituting from (27) and (33) in (29) we obtain an explicit expression for $z(f_a, p)$; then it remains to maximize this with respect to both f_a and p. It is convenient first to fix f_a and maximize with respect to p; the equilibrium value of p is given implicitly by the equation

$$\frac{\partial}{\partial p}\left[\ln g(f_a, p) - \frac{W(f_a, p)}{kT}\right] = 0 \qquad (34)$$

Substituting for $g(f_a, p)$ and $W(f_a, p)$ and performing the partial differentiation the equilibrium value of p is given by the solution of

$$f_a(1-p)(f_b - f_ap) = f_ap\,(1-2n_A + f_ap)\,e^{2J/hkT} \qquad (35)$$

or by reference to Table III

$$\frac{[A \text{ on } a;\ B \text{ on } b]\,[B \text{ on } a;\ A \text{ on } b]}{[A \text{ on } a;\ A \text{ on } b]\,[B \text{ on } a;\ B \text{ on } b]} = e^{2J/hkT} \qquad (36)$$

where each [ ] indicates the number of nearest neighbor pairs in the equilibrium configuration occupied in the manner in-

dicated inside the bracket. This equation has the simple form of quasi-chemical equilibrium from which the method derives its name. It is to be noted that if the right hand side of (36) is replaced by unity the formula becomes that appropriate to a random distribution of the four kinds of pairs for given f_a, and this would lead to the formulas of the zeroth approximation. The two approximations will clearly become equivalent in the limit $h \to \infty$ when it is easily seen that the approximations involved in either method become equivalent.

For simplicity we shall now consider the case of the 50-50 alloy($f_a+f_b=1$, $n_A=n_B=\frac{1}{2}$); the general alloy may be treated in the same manner but the equations are more complex. For the 50-50 alloy (35) becomes

$$(1-p)(1-f_a(1+p)) = f_a p^2 e^{2J/hkT}$$

with the solution(the other solution is negative and hence of no physical interest)

$$p = \frac{[1+4f_a(1-f_a)(e^{2J/hkT}-1)]^{1/2} - 1}{2f_a(e^{2J/hkT}-1)} \qquad (37)$$

giving the equilibrium value of p as a function of the still to be determined equilibrium value of f_a. The equilibrium value of f_a is finally determined by substituting for p from (37) in the partition function (29) and maximizing the function thus obtained with respect to f_a; that is

$$\frac{\partial}{\partial f_a}[\ln g(f_a) - w(f_a)/kT] = 0 \qquad (38)$$

Performing the differentiation and letting

$$\theta = [1 + 4f_a(1-f_a)(e^{2J/hkT}-1)]^{1/2} \qquad (39)$$

it may be shown that the required equilibrium value of f_a is given implicitly by

$$\ln\left(\frac{\theta + 2f_a - 1}{\theta - 2f_a + 1}\right) = \frac{h-2}{h} \ln\left(\frac{f_a}{1-f_a}\right) \qquad (40)$$

From the definition of f_a and S from the previous section it is apparent that

$$f_a = \frac{1+S}{2} \qquad (41)$$

whence (37), (39), and (40) become

$$P = \frac{\theta - 1}{(1+S)(e^{2J/h\mathcal{k}T} - 1)} \qquad (42)$$

$$\theta = [1 + (1-S^2)(e^{2J/h\mathcal{k}T} - 1)]^{1/2} \qquad (43)$$

$$\ln\left(\frac{\theta+S}{\theta-S}\right) = \frac{h-2}{h} \ln\left(\frac{1+S}{1-S}\right) \qquad (44)$$

As before the free energy, F(S), and the configuration energy, E(S), may be obtained from the partition function and are given by

$$\frac{F(S) - F(1)}{(N\mathcal{k}T/2)} = (1+S)\ln(1+S) + (1-S)\ln(1-S) - 2\ln 2 + \frac{h}{2}\left[(1+S)\ln\left(\frac{\theta+S}{1+S}\right) + (1-S)\ln\left(\frac{\theta-S}{1-S}\right) - 2\ln\left(\frac{\theta+1}{2}\right)\right] \qquad (45)$$

and

$$E(S) - E(1) = \frac{NJ}{2}\left(\frac{1-S^2}{1+\theta}\right) \qquad (46)$$

where S is given by the solution to (44). For $J>0$ the critical temperature is determined by (22). The result is

$$\frac{J}{\mathcal{k}T_c} = h \ln\left(\frac{h}{h-2}\right) \qquad (47)$$

which, as we have anticipated, reduces to the Bragg-Williams value for $h\to\infty$. Using (47) the equilibrium value of S as a function of the reduced temperature, T/T_c, may be obtained from (44), the result being

$$S^2\left[1 + \left(\frac{1+S}{1-S}\right)^{\frac{h-2}{h}}\right]^2 = \left[\left(\frac{h}{h-2}\right)^{2\frac{T_c}{T}} - S^2\left(\left(\frac{h}{h-2}\right)^{2T_c/T} - 1\right)\right]\left(1 - \left(\frac{1+S}{1-S}\right)^{\frac{h-2}{h}}\right)^2 \qquad (48)$$

which can be solved numerically for various values of h.

Finally the specific heat can be obtained from (43) and (46) by C=dE/dT which leads to

$$C = \frac{J}{2}\frac{1}{1+\theta}\left[\frac{dS}{dT}\left((1-S^2)(1+\theta)^{-1}\frac{\partial\theta}{\partial S} - 2S\right) + \frac{\partial\theta}{\partial T}(1-S^2)(1+\theta)\right] \quad (49)$$

By using (43) and (44) we obtain finally

$$C = \frac{J}{2}\frac{1}{1+\theta}\left[\frac{(S^2-1)^2}{\theta(1+\theta)}\frac{J}{hkT^2}e^{2J/hkT}\left(\frac{2S^2}{\theta(S^2-\theta^2)}\left(e^{2J/hkT}-1\right)-1\right)\right.$$

$$\left. + \frac{4S^2}{S^2-1}\frac{h-2}{h} + \frac{4S}{\theta+S} + \frac{4S^2}{\theta(\theta^2-S^2)}\left(e^{2J/hkT}-1\right)\right] \quad (50)$$

C. Theory of Distortion Dependent Interaction Energies

In this section a theory of order-disorder is presented which differs from the theories of the two previous sections in that a specific form is assumed for the pairwise interaction energy.[24] In the previous sections the specific form of J_{AA}, J_{BB}, J_{AB} was neglected; and, in particular, their possible variations with composition and lattice parameter of the alloy were ignored. Thus the results derived from these two approximations, (25) and (48), implicitly assume the interaction energies are constant independent of these possible variations. But this is not a physically reasonable assumption since variations in the composition and/or the lattice parameter of the alloy will determine the kinds and numbers of nearest neighbors of a given atom in an alloy, and this certainly influences the form of the pairwise interaction energy. Thus, as a first step towards presenting a physically reasonable description of ordering in alloys, we shall consider the effects of the dependence of the interaction energy on the lattice parameter and variation of the lattice parameter upon the or-

dering in the alloy.

In the first example of this theory we shall consider the case of the body-centered cubic lattice for which a typical example is CuZn or β-brass and is depicted in Figure 3. If we let a_0 be the length of a side of the unit cell in the body-centered cubic lattice, then the separation between the Cu and Zn atoms is given by $x=\sqrt{3}\, a_0/2$. Now the assumption of this theory is that the interaction energies have the following form

$$J_{AA} = \frac{Y}{2}(x-\xi)^2 + K \qquad (51)$$

$$J_{BB} = \frac{Y}{2}(x-\eta)^2 + L \qquad (52)$$

$$J_{AB} = \frac{Y}{2}(x-\rho)^2 + M \qquad (53)$$

where ξ, η, and ρ are the relative displacements of the atoms from the equilibrium positions defined by x.

Now be reference to Table I, for the 50-50 alloy, we have the distribution of A and B atoms on the a and b sites. Then the probabilities for AA, BB, and AB pairs are given by Table IV and the energies of such pairs become

$$J_{AA} = \frac{1-S^2}{4}\left[\frac{Y}{2}(x-\xi)^2 + K\right] \qquad (54)$$

$$J_{BB} = \frac{1-S^2}{4}\left[\frac{Y}{2}(x-\eta)^2 + L\right] \qquad (55)$$

$$J_{AB} = \frac{1+S^2}{4}\left[\frac{Y}{2}(x-\rho)^2 + M\right] \qquad (56)$$

We now write the configuration energy as

$$W = \frac{S^2}{2}\left[\frac{Y}{4}\left[2(x-\rho)^2 - (x-\xi)^2 - (x-\eta)^2 + M - \frac{K}{2} - \frac{L}{2}\right]\right] + \frac{1}{2}\left[\frac{Y}{4}\left(2(x-\rho)^2 + (x-\xi)^2 + (x-\eta)^2 + M + \frac{K}{2} + \frac{L}{2}\right)\right] \qquad (57)$$

The configuration energy is now minimized with respect to the equilibrium position, x, in order to obtain the equilibrium configuration. We have

$$\frac{\partial W}{\partial \chi} = 0$$

which gives the result

$$\chi = \frac{S^2}{4}(2\rho - \xi - \eta) + \frac{2\rho + \xi + \eta}{4} \qquad (58)$$

or letting

$$\chi_0 = \frac{2\rho + \xi + \eta}{4}, \quad \chi' = \frac{2\rho - \xi - \eta}{4} \qquad (59)$$

then we have

$$\chi = \chi_0 + \chi' S^2 \qquad (60)$$

which implies that the equilibrium position of the atoms in the alloy depends upon the state of order in the alloy. If we now substitute for x from (60) into (57) we have

$$W = \phi + QS^2 + PS^4 \qquad (61)$$

where

$$\phi = \frac{Y}{2}\left[\frac{1}{2}\left(\rho^2 + \frac{\xi^2+\eta^2}{2}\right) + M + \frac{L+K}{2} - \chi_0^2\right]$$

$$Q = \frac{Y}{2}\left[\frac{1}{2}\left(\rho^2 - \frac{\xi^2+\eta^2}{2}\right) + M - \frac{L+K}{2} - 2\chi_0\chi'\right]$$

$$P = -\frac{Y}{2}(\chi')^2$$

The Helmholtz free energy may be written as

$$F = W - TS' \qquad (62)$$

and the entropy, S', may be written[25]

$$S' = -k\left(\frac{1+S}{2}\ln\left(\frac{1+S}{2}\right) + \frac{1-S}{2}\ln\left(\frac{1-S}{2}\right)\right) \qquad (63)$$

Using (61) and (63) in (62) we obtain

$$F = \phi + QS^2 + PS^4 + kT\left(\frac{1+S}{2}\ln\left(\frac{1+S}{2}\right) + \frac{1-S}{2}\ln\left(\frac{1-S}{2}\right)\right) \qquad (64)$$

Again using (22) we obtain

$$\frac{kT}{I} = \frac{2S(1+DS^2)}{\ln\left(\frac{1+S}{1-S}\right)} \qquad (65)$$

where we have let I=-2Q and D=P/Q. We now define $I=kT_c$ so that (65) becomes

$$\frac{T}{T_c} = \frac{2S(1+DS^2)}{\ln\left(\frac{1+S}{1-S}\right)} \qquad (66)$$

If we now expand the logarithmic term we have

$$\frac{T}{T_c} = \frac{2S(1+DS^2)}{2S(1+\frac{S^2}{3}+\ldots)} \qquad (67)$$

or

$$\frac{T}{T_c} = 1 + S^2(2D-\tfrac{1}{3}) + \ldots \qquad (68)$$

Finally, considering the configurational specific heat, we obtain in a manner similar to (26)

$$C = \frac{k}{2}\frac{T}{T_c}\left[\ln^2\left(\frac{1+S}{1-S}\right)\Big/\left[\frac{4S(1+DS^2)}{(1-S^2)\ln\left(\frac{1+S}{1-S}\right)} - 2 - 6DS^2\right]\right] \qquad (69)$$

In this section we shall apply this theory to an alloy such as CoPt which when ordered assumes the face-centered tetragonal structure such as is depicted in Figure 12 in the 50-50 composition.

The Platinum atoms are situated at $(0,0,0)$ and $(\frac{1}{2},\frac{1}{2},0)$ while the Cobalt atoms are at $(\frac{1}{2},0,\frac{1}{2})$ and $(0,\frac{1}{2},\frac{1}{2})$. There are two lattice parameters in this structure; the "a" parameter which we shall take to be the length of the unit cell along the x and y-axes, and the "c" parameter which we shall take to be the length of the unit cell along the z-axis. Thus it can be seen that there will be two types of nearest neighbor pairs; one type shall be called 'a' pairs of which there are four separated by the distance $a/\sqrt{2}$ and the other type shall be called 'c' pairs for which there are eight separated by a distance $(a^2+c^2)^{\frac{1}{2}}/2$.

We shall let $(1+S)/2$ be the probability that a site is correctly occupied whether it is a site involving an 'a' pair or a 'c' pair. Then for 'a' pairs the probabilities for AA, BB, and AB pairs whether they are Cobalt or Platinum are given in Table V where ϵ is a normalization constant

to be determined. For 'c' pairs the results are given in Table VI. Now ϵ is determined from the condition that the sum of all the probabilities equals unity. This gives $\epsilon=6$. Again the interaction energies are given by (51)-(53). Then the energies of the 'a' pairs become

$$J_{AA} = \frac{1+S^2}{12}\left[\frac{Y}{2}\left(\frac{a}{\sqrt{2}} - \beta\right)^2 + K\right] \qquad (70)$$

$$J_{BB} = \frac{1+S^2}{12}\left[\frac{Y}{2}\left(\frac{a}{\sqrt{2}} - \eta\right)^2 + L\right] \qquad (71)$$

$$J_{AB} = \frac{1-S^2}{6}\left[\frac{Y}{2}\left(\frac{a}{\sqrt{2}} - \rho\right)^2 + M\right] \qquad (72)$$

Then the configurational energy for 'a' pairs is

$$W_a = \frac{S^2}{12}\left[\frac{Y}{2}\left(\frac{a}{\sqrt{2}} - \beta\right)^2 + \frac{Y}{2}\left(\frac{a}{\sqrt{2}} - \eta\right)^2 - Y\left(\frac{a}{\sqrt{2}} - \rho\right)^2 + K + L - 2M\right]$$
$$+ \frac{1}{12}\left[\frac{Y}{2}\left(\frac{a}{\sqrt{2}} - \beta\right)^2 + \frac{Y}{2}\left(\frac{a}{\sqrt{2}} - \eta\right)^2 + Y\left(\frac{a}{\sqrt{2}} - \rho\right)^2 + K + L + 2M\right] \qquad (73)$$

We again minimize the configurational energy with respect to the parameter "a" in order to obtain the equilibrium configurational energy corresponding to the equilibrium structure parameter. Then

$$\frac{\partial W_a}{\partial a} = 0$$

gives

$$a = \frac{\sqrt{2}}{4}(\beta + \eta + 2\rho) + \frac{\sqrt{2}}{4}S^2(\beta + \eta - 2\rho) \qquad (74)$$

or letting

$$a_0 = \frac{\sqrt{2}}{4}(\beta + \eta + 2\rho), \quad a_1 = \frac{\sqrt{2}}{4}(\beta + \eta - 2\rho)$$

we have

$$a = a_0 + a_1 S^2 \qquad (75)$$

which is similar to (60). Now for the 'c' pairs the interaction energies may be written

$$J_{AA} = \frac{1-S^2}{6}\left[\frac{Y}{2}(d - \beta)^2 + K\right] \qquad (76)$$

$$J_{BB} = \frac{1-S^2}{6}\left[\frac{Y}{2}(d - \eta)^2 + L\right] \qquad (77)$$

$$J_{AB} = \frac{1+S^2}{3}\left[\frac{Y}{2}(d - \rho)^2 + M\right] \qquad (78)$$

where

$$d = (a^2 + c^2)^{1/2}/2$$

Again we write the configurational energy of the 'c' pairs and minimize it with respect to the parameter d. The result is

$$d = \frac{1}{\sqrt{2}} (a_0 - a_1 S^2) \qquad (79)$$

If we now write

$$a = a_0 (1 + \delta_0) \qquad (80)$$

and

$$c = a_0 (1 - \delta_1) \qquad (81)$$

where δ_0 and δ_1 are small, that is δ_1, $\delta_0 << 1$; then (80) and (81) become

$$a_0 (1 + \delta_0) = a_0 + a_1 S^2 \qquad (82)$$

and

$$a_0 (2 - 2\delta_1 + 2\delta_0 + \delta_1^2 + \delta_0^2)^{1/2} = \sqrt{2} (a_0 - a_1 S^2) \qquad (83)$$

and to first order in the deltas (83) becomes

$$a_0 (1 - (\delta_1 - \delta_0))^{1/2} = a_0 - a_1 S^2 \qquad (84)$$

or by expanding the exponent

$$a_0 (1 - \tfrac{1}{2} (\delta_1 - \delta_0)) \simeq a_0 - a_1 S^2 \qquad (85)$$

Solving (80) and (85) for δ_0 and δ_1 we have

$$\delta_0 = \frac{a_1}{a_0} S^2 \quad , \quad \delta_1 = 3 \frac{a_1}{a_0} S^2 \qquad (86)$$

Therefore

$$\frac{c}{a} = \frac{1 - \delta_1}{1 + \delta_0} \approx (1 - \delta_1)(1 - \delta_0) \approx 1 - 4 \frac{a_1}{a_0} S^2 \qquad (87)$$

or

$$1 - \frac{c}{a} \propto 4 \frac{a_1}{a_0} S^2 \qquad (88)$$

The departure, or distortion, from face-centered cubic sy-

mmetry, and consequent assumption of face-centered tetragonal symmetry, may be expressed quantitatively by the quantity 1-(c/a). Equation (88) gives us the key result of this theory, that this distortion is proportional to the order parameter squared; and therefore gives us a convenient experimental method of measuring the order parameter.

The volume of the unit cell is

$$V = c a^2$$

which becomes

$$V = a_0^3 (1 - \delta_1)(1 + \delta_0)^2 \approx a_0^3 (1 - \delta_1 + 2\delta_0) \qquad (89)$$

or

$$V \approx V_0 \left(1 - 3\frac{a_1}{a_0} S^2 + 2\frac{a_1}{a_0} S^2\right) = V_0 \left(1 - \frac{(1 - \frac{c}{a})}{4}\right) \qquad (90)$$

By considering the Helmholtz free energy, (62), and the entropy, (63), we will again obtain (66) and for the specific heat (69).

D. Exact Expansions of the Free Energy

As we have mentioned before order-disorder transitions are but one manifestation of what might be called critical phenomena. Recently there has been much work done in attempting to deal with the mathematical difficulties encountered in working with such models as the Ising model. To begin with, a solution to the two-dimensional Ising model for a plane-square lattice has been given by Onsager[26] by a matrix formulation and alternatively by Green and Hurst[27] by the method of the Pfaffian. These methods have been applied to other types of lattices such as the triangular

and honeycomb. These results have the feature that the free energy assumes a non-Taylor like expansion form such as[28]

$$F(T) = F_c + a(T-T_c) + b(T-T_c)^2 \ln|T-T_c| + \ldots \quad (91)$$

where a and b are constants. Various phenomenological and classical attempts write the free energy as an expansion in such thermodynamic properties as the temperature or magnetization, obtain the coefficients of the expansion by expanding them in powers of $(T-T_c)$, and finally obtain the magnetization as a function of T_c-T.[29] If we define the spontaneous magnetization as

$$M_0(T) = \lim_{H \to 0^+} M(H,T)$$

then the phenomenological theories predict

$$M_0(T) \simeq (T-T_c)^{\beta} \quad (92)$$

and

$$C_{H=0}(T) \simeq \begin{cases} (T-T_c)^{-\alpha} & (T>T_c) \\ (T_c-T)^{-\alpha'} & (T<T_c) \end{cases} \quad (93)$$

where $C_{H=0}$ is the specific heat in zero magnetic field and β, α, and α' are exponent constants. The exact results from the two-dimensional Ising model has given[30]

$$\alpha = \alpha' = 0 \quad , \quad \beta = \frac{1}{8} \quad (94)$$

For the three-dimensional Ising model such expansions are also attempted, some in the form

$$F(T) = \sum_{n=0}^{\infty} f_n (kT)^{-n} \quad (95)$$

and are applied to such lattices as the simple cubic, body-centered cubic, and face-centered cubic. The results of such expansions to a considerable number of terms gives confidence that the results for the three-dimensional Ising model are[31]

The results of the theory presented in section C, which we may call a "mean field" theory, would give[32]

$$\alpha = \alpha' = 0 \quad , \quad \beta = \tfrac{1}{2} \qquad (97)$$

From (60), (75), and (79) we should note that the "mean field" theory predicts that the lattice may experience distortions such as contractions and elongations. In a very illuminating paper Baker and Essam[33] have formulated a partition function which incorporates both elastic degrees of freedom and an orderable spin system. They considered the simple cubic structure and showed that their model reduced to the solution of the rigid-lattice Ising model. It is interesting to note that part of the interactions they chose were of a form similar to (51)-(53). Their model does not undergo a first-order transition at the critical point. Their model exhibits exponent renormalization in that below the critical temperature α' and β are given by (96) while above the critical temperature

$$\alpha' \rightarrow \frac{-\alpha'}{1-\alpha'} \quad , \quad \beta \rightarrow \frac{\beta}{1-\alpha'} \qquad (98)$$

This change in exponents would mean that the specific heat has a finite, cusp-shaped peak and would not appear to increase indefinitely incontrast, say, to Figure 4. Finally, the difficulties with this model, as pointed out by Guttman[34], are that the size of the effects stressed by Baker and Essam, namely rounding of the specific heat and exponent renormalization are very difficult to observe until $1-(T/T_c)$

$\approx \mathcal{O}(10^{-50})$. This point raises at least two questions which are: first, the thermodynamic stability can be thought of as resulting from the close cancellation of two large, but not infinite, terms. Will a more general model yield first-order transitions or renormalized exponents depending on the model parameters? Next, over what range of temperatures is renormalization important and when, if ever, does the specific heat show which exponent?[35]

III. Experimental Procedure

A. Alloy preparation

The CoPt alloy was prepared from samples of Cobalt and Platinum which were 99.9 and 99.9995% pure respectively. The Cobalt metal was cleaned by washing in acetone, then 1M HNO_3, distilled water, and finally again in acetone. The metals were then melted together in an argon arc melting furnace(Materials Research Corp. model AF-92C). Oxygen (and any other gas) contamination was minimized by melting a piece of Titanium metal at the same time. The metals were weighed preceding the melting and the alloy after the melting. Thus the composition range of the alloy was 49.75 to 50.08 atomic per cent Cobalt. The alloy was then placed in Vycor tubing attached to the vacuum system, pumped down to a pressure of 1.3×10^{-5} torr, filled with argon to 160 torr, and sealed off. The alloy was placed in the furnace for a homogenization anneal at 1000 °C for 100 hours. At the end of the 100 hours the sample was removed from the furnace by means of Kanthal tongs and quenched in an ice-water bath at 0 °C.

B. Vacuum system

In order to bring about the ordered phase of the CoPt it is necessary to heat treat or anneal the alloy. Thus it became necessary to construct a vacuum system for use in evacuating Vycor tubing. The vacuum system allowed the Vycor tubing to be evacuated and then filled with an inert gas such as argon so that during the annealing process the

alloy would not undergo oxidation. The system used an Edwards model E01 oil diffusion pump and typical pressures were of the order of 10^{-6} torr in an air atmosphere.

C. Furnace and Controlling system

Two annealing furnaces were constructed using Kanthal heating elements and components(model REH 7-60). The heat zone of the furnaces was calibrated using a thermocouple encased in an alumina sheath. Subsequent to the calibration all enclosed samples were positioned in the furnace by means of an L-shaped steel rod so that they were always in the hottest portion of the heat zone to minimize thermal fluctuations.

The temperature controlling system for the furnace is shown in Figure 16. The controlling element is a thermocouple(Leeds&Northrup Chromel-Alumel) placed closely adjacent to the sample situated in the furnace. The e.m.f. of the thermocouple is balanced by a poteniometer(Leeds& Northrup model 8696); the difference in e.m.f. between the desired annealing temperature and the actual furnace temperature actuates a galvanometer(Pye model 7891/S) whose sensitivity is 8 μV/mm. The light spot reflected from this galvanometer falls on either of two cadmium-selenide photocells which control the furnace current through a relay circuit. If the furnace temperature is too high cell 1, C_1 in Figure 17, is illuminated causing the relay arm to move which reduces the furnace current by approximately 5 amperes since there is a voltage drop, V_d in Figure 16, of

20 volts across the transformer primary(General Radio Corp. model W50). When the furnace temperature cools, cell 2, C_2 in Figure 17, is illuminated and the furnace current increases by about 4.5 amperes.

The relay controlling circuit is shown in Figure17. The two capacitors, C, had a value of 40 μfarads, V_{out}=42 volts, the two resistors R had the value of 62 kΩ each, and the two transistors T were Westinghouse type n-p-n 2N4922.

The chromel-alumel thermocouple used in the furnace control system was calibrated by fitting the observed e.m.f. produced when measuring the known melting temperatures of various substances to an equation of the form

$$E = a + bT + cT^2 + \ldots$$

where E is the observed e.m.f., T is the observed temperature, a, b, and c are constants to be determined.[36] The constants a, b, and c were determined by measuring the melting points of KCl and LiCl and the boiling point of distilled water. Then a new set of constants m, n, and p were determined from the equation

$$E' = m + nT + pT^2$$

by using the tabulated values for the melting and boiling points of the aforementioned substances.[37] Then the e.m.f. corresponding to the desired annealing temperature was calculated from

$$E_{anneal} = E_{tables} + E''$$

where

$$E'' = E - E'$$

By positioning the photocells C_1 and C_2 about 1 cm from the center position of the galvanometer light and letting .04mV=1 ^{o}C for a chromel-alumel thermocouple the final range of control was approximately $\pm$ 2 ^{o}C.

D. X-ray measurements

After the alloy had been homogenized filings were made from the alloy using an Al_2O_3 grinding wheel. The filings were separated from the Al_2O_3 powder by means of a magnet, placed in Vycor tubing cleaned with acetone, evacuated and then filled with a partial pressure of argon such that the pressure inside the tube would equal 760 torr at the temperature of anneal, and sealed off. The sealed off tube was then situated in the calibrated heat zone of the furnace and annealed. At the end of each anneal the sample was quickly removed from the furnace and quenched in an ice-water bath at 0 ^{o}C. The filings were then removed from the tube and mounted on a glass capillary which was positioned in the center of a 114.6 mm diameter Debye-Scherrer X-ray powder camera. The film was loaded in the Straumanis-Ievins arrangement. The X-ray beam was obtained from a Phillips model PW 1011 X-ray generator. The X-ray tube was an Fe tube with a Mn filter so that the beam consisted of the FeKα radiation. Exposure times to the beam varied between 3 to 4 hours. After film development measurements of the lattice parameter were made with the use of a Picker-Nuclear X-ray film reader. The procedure followed in measuring the lines consisted of locating the center of a line in the

photograph with respect to the left edge of the film reader to within ± .001 mm. This procedure was done for all the lines visible in a photograph and each line was measured at least 10 times. To check the accuracy of these measurements, any two lines corresponding to a given index, for example the (110) lines, had their two values added together and divided by 2. The result gave the position of the $2\theta=0^\circ$ hole in the film on the film reader. This procedure was done for other lines, such as the (111), (200), and (112), which bracketed the $2\theta=0^\circ$ hole. Similarly the same procedure was carried out for lines such as the (221), (311), (222), and (203) which bracketed the $2\theta=180^\circ$ hole. If the disagreement between these measurements for the location of the two positions on the film reader was greater than ± .005 mm, the lines were re-measured another five times and the procedure was repeated until the various measurements agreed to within ± .005 mm. With the radiation used the following lines were obtained in the ordered phase and measured(in order of increasing θ): (001), (110), (111), (200), (002), (201), (112), (202), (220), (221), (003), (310), (311), (113), (222), (203), and (132).

Using the assigned indices of the lines of the photograph and the values of the spacings between the lines of a given index the value of and hence sin is calculated from

$$\theta = \frac{(x_2 - x_1)}{2} \times \text{film shrinkage factor}$$

where x_2 and x_1 are the two lines corresponding to a given lattice index and the film shrinkage factor is calculated

by subtracting the measured position on the film reader of the $2\theta=0^{\circ}$ hole from the measured position of the $2\theta=180^{\circ}$ hole and then dividing the result by 180 mm which is the value of the subtraction if there were no film shrinkage.

Now for a tetragonal system the spacing between lattice planes is given by

$$\frac{1}{d^2} = \frac{h^2 + k^2}{a^2} + \frac{l^2}{c^2}$$

where h,k,l is the index of a lattice plane and a and c are the unit cell parameters. Then using the Bragg equation

$$\lambda = 2 d \sin \theta$$

we have

$$\left(\frac{a}{c}\right)^2 = \frac{4 \sin^2 \theta}{\lambda^2 a^2} - \frac{h^2 + k^2}{l^2}$$

and

$$a^2 = \frac{\lambda^2 (h^2 + k^2)}{4 \sin^2 \theta} \qquad (\text{for } hk0 \text{ planes})$$

Following the direct graphical method of Myers and Davies[38] we assume at least two different values for $(a/c)^2$ and solve the equation for a^2. A straight line of $(a/c)^2$ plotted against a^2 is obtained for each lattice plane. Such a plot is shown in Figure 18 for a sample annealed at 800°C for 48 hours. Ideally, without drift or scatter, the lines should intersect at a common point. Since it isknown that the drift is greatest at the lower angles and decreases as θ approaches 90°, it is apparent that the line of best fit would have to intersect the diffraction peak lines in a definite sequence, that is from the lower angle lines to the higher angle lines in regular succession. Thus a straight edge was placed over each plot horizontally and adjusted

vertically until the lines appeared to be intersecting the straight edge in the proper order. Thus an extrapolated value for $(a/c)^2$ was obtained. This value was then substituted in the equation for $(a/c)^2$ above and a value of a^2 was calculated. These values of a^2 for each lattice index were then plotted against the Nelson-Riley function and the best straight line drawn through them gave an extrapolated value of a^2 corresponding to $\theta=90^\circ$. Thus a and c were separately calculated.

In order to determine when a sample which had been annealed was exhibiting the equilibrium degree of order appropriate to that annealing temperature, the X-ray photographs were examined for resolution of the $\alpha_1-\alpha_2$ lines in the highest angle of diffraction, that is the (132) line. If the $\alpha_1-\alpha_2$ resolution was not exhibited, then it was assumed that the sample was not in equilibrium and the sample was re-annealed and the subsequent photograph examined for the $\alpha_1-\alpha_2$ resolution. This procedure was repeated until the resolution was obtained. Naturally a sample which was annealed for a time t_1 exhibited different lattice parameters than the same sample after annealing for a time $t_2=t_1+\tau$. As an example, the sample annealed for 24 hours at 800°C had an extrapolated a=3.798 Å and c=3.697 Å while the same sample after being annealed for an additional 24 hours at the same temperature for a total of 48 hours had a=3.796 Å and c=3.701 Å.

With an estimated error in the film readings of $\pm$ .001

mm this would give an estimated error in the measurement of d of $\pm$ .003 A.

Finally, in Table VII are listed the anneal times, temperatures, and the values of a, c, and c/a which are used in Figure 22.

IV. Results and Discussion

The results of the Bragg-Williams, quasi-chemical, the present theory, and the compressible Ising model theory as applied to the body-centered cubic alloy CuZn are presented in Figure 19. Also presented in Figure 19 are the experimental results of Norvell and Als-Nielsen[39] represented by an o, and the experimental results of Chipman and Walker[40] represented by a ∇. The results of Norvell and Als-Nielsen were obtained by a neutron diffraction experiment measuring the peak intensities of the superlattice reflections. The results of Chipman and Walker were obtained from X-ray measurements of the integrated intensities of the superlattice reflections. Chipman and Walker claim the results of Norvell and Als-Nielsen are in error since (1) Norvell and Als-Nielsen did not recognize the large difference in the values of the Debye-Waller exponents for Cu and Zn upon which the intensity of the superlattice reflection depends, that is

$$I \simeq S^2 \left| f_{Zn} \exp(-M_{Zn}) - f_{Cu} \exp(-M_{Cu}) \right|^2$$

where f is the scattering factor of the atom and M is its Debye-Waller exponent, proportional to its mean square amplitude of thermal vibration, and (2) their corrections for extinction are large. In the region of $T/T_c > .97$ the Ising model predicts that the long-range order parameter follows a power law, that is

$$S \simeq D\,(1 - T/T_c)^{\beta}$$

where the measured values of D and β are 1.49 and .293

respectively. Chipman and Walker claim that in this region their measurements are not yet sufficient to make quantitative comparisons but that outside this region, that is $T/T_c < .97$, their measurements differ considerably from the predictions of the Ising model and the difference, in part, may be due to the long range interactions that characterize real alloys rather than the assumption of nearest neighbor interactions only of Baker and Essam.[33] The result of the present theory is clearly a poorer approximation to the experimental values than the compressible Ising model and may, in part, be due to the assumption of equations (51)-(53) for the interaction energies.

In Figure 20 are shown the results for the specific heat of β-brass, CuZn. The experimental values are from Sykes and Wilkinson.[41] The agreement between the present theory and the experimental values is quite good although the failing of the present theory is that the specific heat drops to the value expected for lattice vibration effects only for $T>T_c$ while the experimental values show the effect on the specific heat of short-range order persisting beyond the critical temperature. In this respect the quasi-chemical theory is more appropriate than the present theory since it predicts the existence of short-range order and its influence on the specific heat beyond the critical temperature.

Figure 21 shows the results of the present experiment on CoPt for equation (90). The value of V_o was obtained

from an X-ray photograph taken of a sample annealed for 12 hours at 1000°C. The value of a_o was extrapolated to be 3.765 Å. The result of Figure 21 is that the volume of the unit cell is constant. The value of the largest discrepancey is only .15%. Thus the prediction of equation (90) is incorrect. One might add on to equation (73) a term of the from $\lambda a^2 c$, where λ is a Lagrangian multiplier, and then proceed to minimize the interaction energies. However, no result comparable to equations (75) and (79) is obtained because the equations for a and c become algebraically coupled. Only by drastic assumptions can (75) and (79) then be re-obtained.

In Figure 22 are depicted the theoretical and experimental results of the long-range order parameter for CoPt. The experimental values represented by an o were obtained in the present experiment. It should be noted that X-ray photographs were taken of samples that had been annealed for temperatures greater than 815°C. However, the superlattice lines that did appear were yet too faint in intensity to be measured with the X-ray film reader. The highest temperature that a sample was annealed that exhibited the lines was 825°C. Since no samples were annealed at temperatures between 825°C and 833°C, it is assumed that the critical temperautre was the value extrapolated by Rudman and Averbach, that is 833°C. The experimental values represented by an x were obtained from the work of Rudman and Averbach.[42] Also from their measured values of c/a are

are obtained the experimental values represented by a . . The theoretical curve was calculated from equation (66) with the aid of the tabulated values of $2S/\ln((1+S)/(1-S))$ by Darby.[43] The comparison between the theoretical curve and the measurements of Rudman and Averbach and the present experiment is qualitatively good. However, the present theory, as represented by equations (51)-(53) has, at best, limited applicability when compared, for example, with the compressible Ising model. One interesting test of the present theory would be to compare equation (69) with experimentally determined values of the specific heat of CoPt. So far no measurements have been made of the specific heat of CoPt. Alternatively, experimental measurements might be made of the long-range order parameter of other binary alloy systems which when ordered exist in the tetragonal phase such as, for example, the Cu-Au alloy system in order to see how well they compare with the theoretical curve in Figure 22.

APPENDIX

The long-range order parameter may be measured by X-ray diffraction techniques since the intensity of the diffraction lines due to the long-range order depends upon the long-range order. This result will be derived by the following consideration. Let r_a be the fraction of $\underline{a}$ sites occupied by A atoms, w_a the fraction of $\underline{a}$ sites occupied by B atoms; similarly for the $\underline{b}$ sites. This distribution is the same as Table I. Then the structure factor for scattering of X-rays is given by

$$F = \sum_{\underline{a}} (r_a f_A + w_a f_B)\, e^{2\pi i (hx + ky + lz)} + \sum_{\underline{b}} (r_b f_B + w_b f_A)\, e^{2\pi i (hx+ky+lz)}$$

where h,k, and l are integers indexing the lattice planes. For CoPt the $\underline{a}$ sites are (0,0,0) and $(\frac{1}{2},\frac{1}{2},0)$ and the $\underline{b}$ sites are $(\frac{1}{2},0,\frac{1}{2})$ and $(0,\frac{1}{2},\frac{1}{2})$. Then F becomes

$$F = \left(\frac{1+S}{2} f_A + \frac{1-S}{2} f_B\right)\left(1 + e^{\pi i (h+k)}\right) + \left(\frac{1+S}{2} f_B + \frac{1-S}{2} f_A\right)\left(e^{\pi i (h+l)} + e^{\pi i (k+l)}\right)$$

It is easily seen that there are only two cases to consider: (1) h+k is even and h,k,l are mixed, that is both even and odd; (2) h+k is even and h,k,l are unmixed, that is either all odd or all even. The first case gives

$$F = 2S\,(f_A - f_B)$$

which will result in the superlattice lines until S=0 when these lines disappear; and the second case gives

$$F = 2\,(f_A + f_B)$$

which are the fundamental lines and are unaffected by the degree of order.

REFERENCES

1. T. Muto and Y.Takagi, Solid State Physics, 1, 193, (1955)

2. K. Huang, Statistical Mechanics, J. Wiley & Sons Inc., Chapter 16, (1963)

3. T. Eguchi et al., Japanese J. Appl. Phys., 5, 645, (1966)

4. E.W. Elcock, Order-Disorder Phenomena, Methuen & Co. Ltd., 26, (1956)

5. C. Kittel, Introduction to Solid State Physics, J. Wiley & Sons Inc. 3rd ed., 218, (1966)

6. F.W. Jones and C. Sykes, Proc. Roy. Soc., A166, 377, (1938)

7. E.W. Elcock, Order-Disorder Phenomena, Methuen & Co. Ltd., 33, (1956)

8. C. Kittel, Introduction to Solid State Physics, J. Wiley & Sons Inc. 3rd ed., 211-212, (1966)

9. J.E. Goldman, Revs. Modern Phys., 25, 108, (1953)

10. S. Siegel, Phys. Rev., 57, 537, (1940)

11. A.S. Darling, Platinum Metals Rev., 7, 96, (1963)

12. J.B. Newkirk et al., J. Appl. Phys., 22, 295, (1951)

13. E. Gebhardt and W. Koster, Z. Metallkunde, 32, 253, (1940)

14. R. Hultgren and R. Jaffe, J. Appl. Phys., 12, 501, (1941)

15. J.B. Newkirk et al., J. Appl. Phys., 22, 290, (1951)

16. A.S. Darling, Platinum Metals Rev., 7, 98, (1963)

17. R.A. Oriani, Acta Met., 1, 144, (1953)

18. J.B. Newkirk et al., J. Appl. Phys., 22, 294, (1951)

19. W. Jellinghaus, Z. tech. Physik, 17, 33, (1936)

20. D.S. Craik and F. Nunez, Proc. Phys. Soc., 78, 225, (1961)

21. J.C. Woolley and B. Bates, J. Less Common Metals, 2, 11, (1960)

22. W.L. Bragg and E.J. Williams, Proc. Roy. Soc. London, A145, 699, (1934)

23. E.W. Elcock, Order-Disorder Phenomena, Methuen & Co. Ltd., 91, (1956)

24. P. Gaunt and P. Tivin, Bull. Am. Phys. Soc., 15, 774, (1970)

25. F. Reif, Statistical and Thermal Physics, McGraw-Hill Co., 219, (1965)

26. K. Huang, Statistical Mechanics, J. Wiley & Sons Inc., Chapter 17, (1963)

27. H. Green and C. Hurst, Order-Disorder Phenomena, Interscience Publishers, Chapter 3, (1964)

28. M.E. Green, Rept. Progr. Phys., 30, 668, (1967)

29. Ibid., 660

30. Ibid., 669

31. Ibid., 692

32. C. Domb, Ann. Acad. Fennicae Ser.A, VI, 174, (1966)

33. G. Baker and J. Essam, Phys. Rev. Letts., 24, 447, (1970)

34. L. Guttman, Phys. Rev. B, 2, 1432, (1970)

35. G. Baker and J. Essam, Phys. Rev. Letts., 24, 449, (1970)

36. A.I. Dahl ed., Temperature, Its Measurement and Control in Science and Industry, Rheinhold Publ. Corp., 3, Part 2, (1962)

37. Handbook of Chemistry and Physics, Chemical Rubber Co., 51st ed., (1970)

38. E. Myers and F.C. Davies, Acta Cryst., 14, 194, (1961)

39. J.C. Norvell and J. Als-Nielsen, Phys. Rev. B, 2, 277, (1970)

40. D.R. Chipman and C.B. Walker, Phys. Rev. Letts., 26, 233, (1971)

41. C. Sykes and H. Wilkinson, J. Inst. Metals, 61, 223, (1937)

42. P.S. Rudman and B.L. Averbach, Acta Met., 5, 65, (1957)

43. M.I. Darby, British J. Appl. Phys., 18, 1415, (1967)

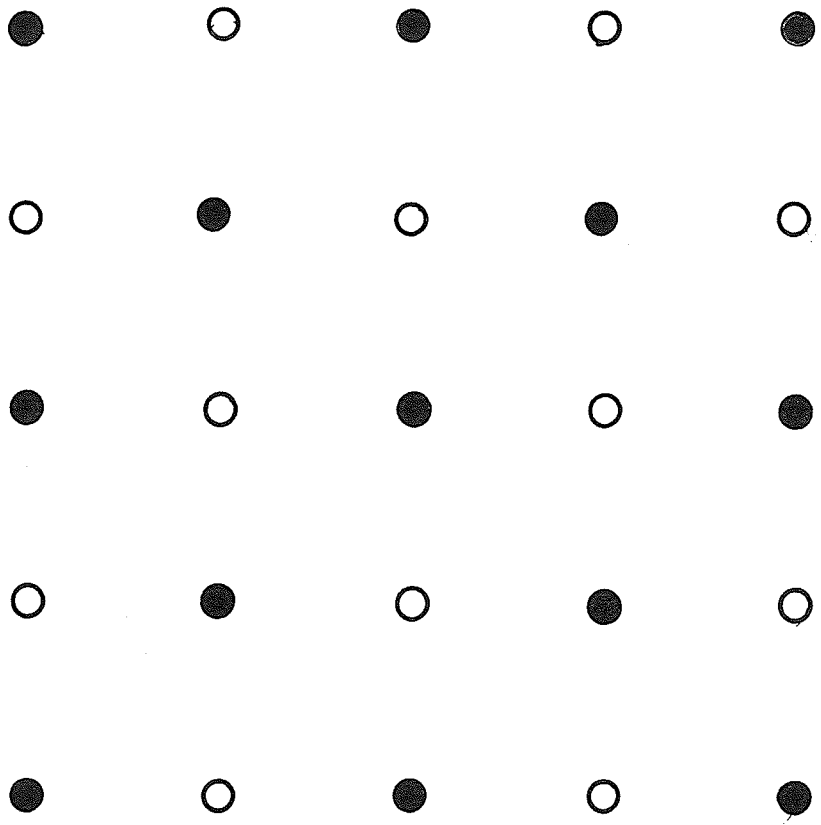

Figure 1

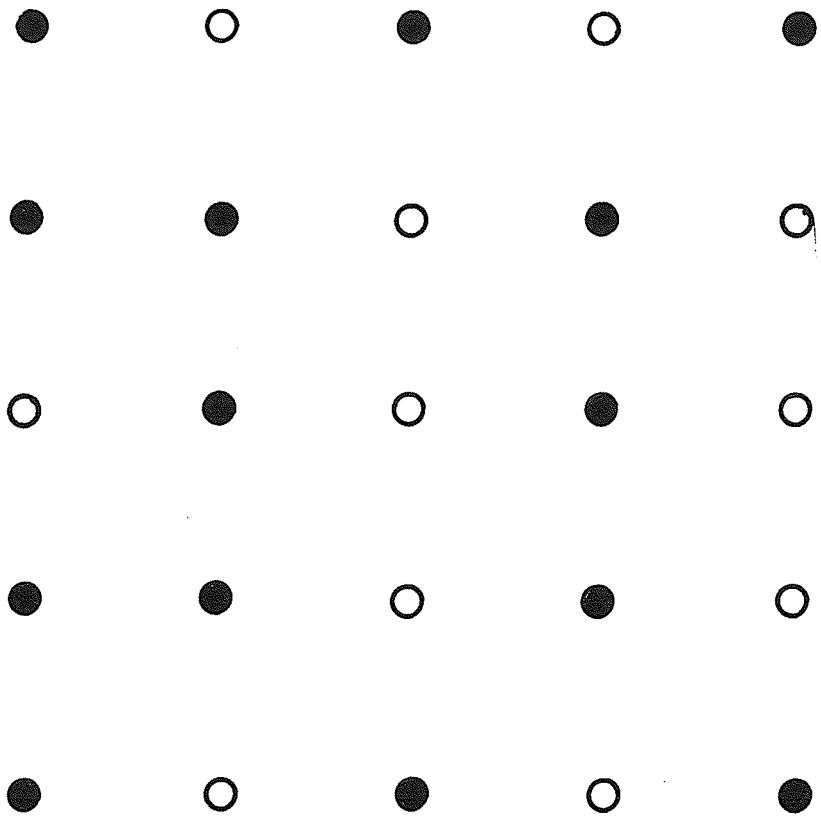

Figure 2

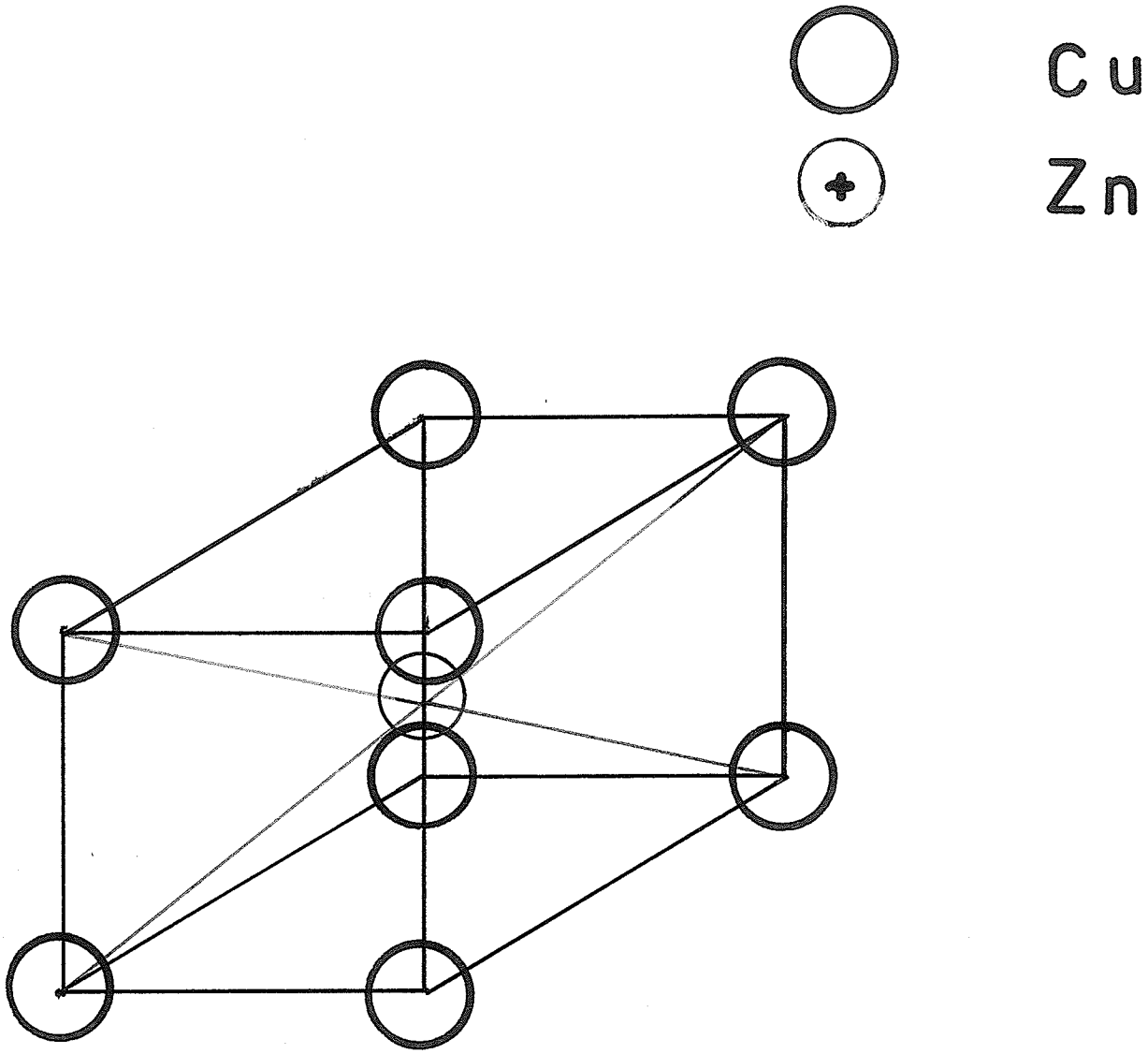

Figure 3

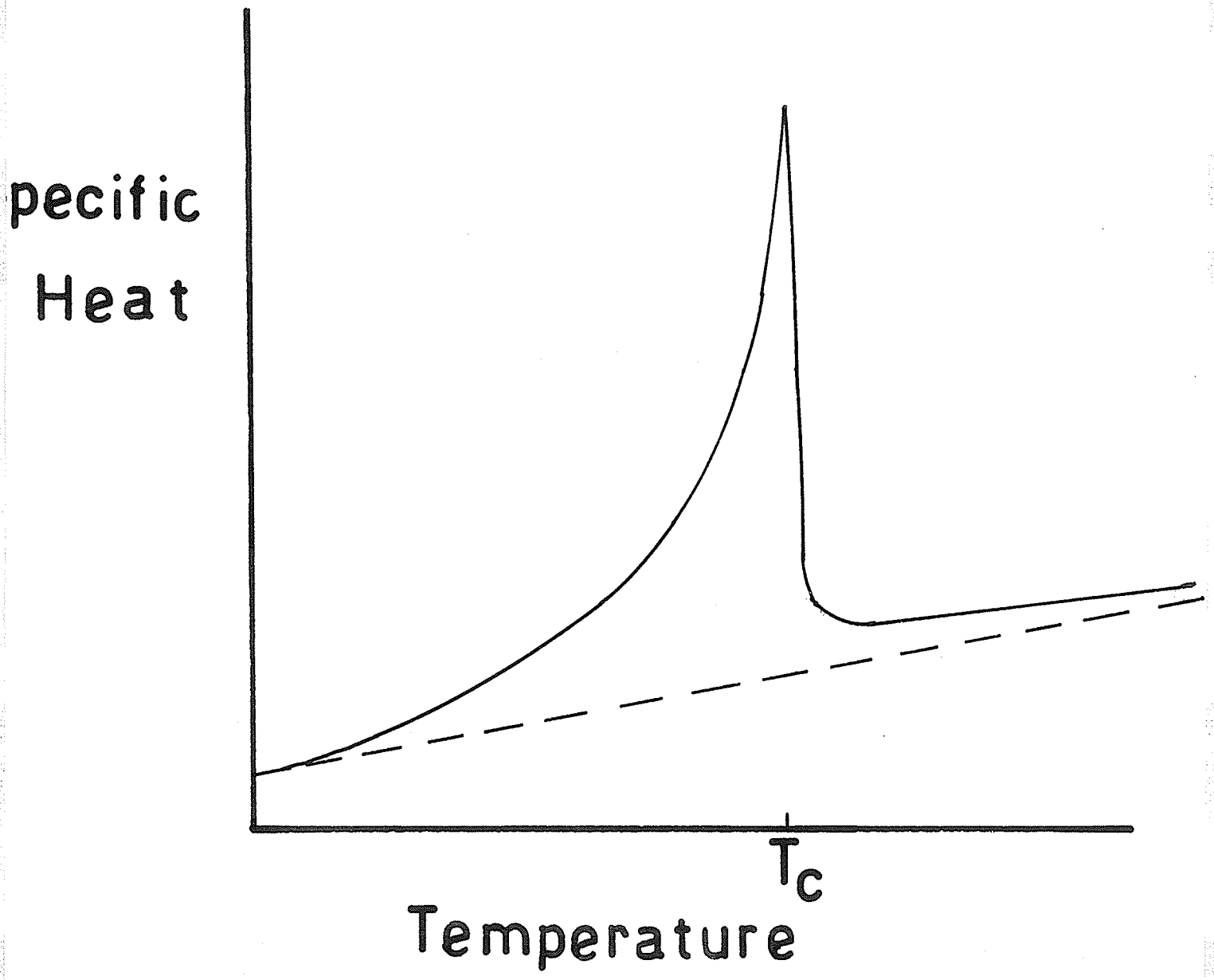

Figure 4

Resistivity of Cu_3Au

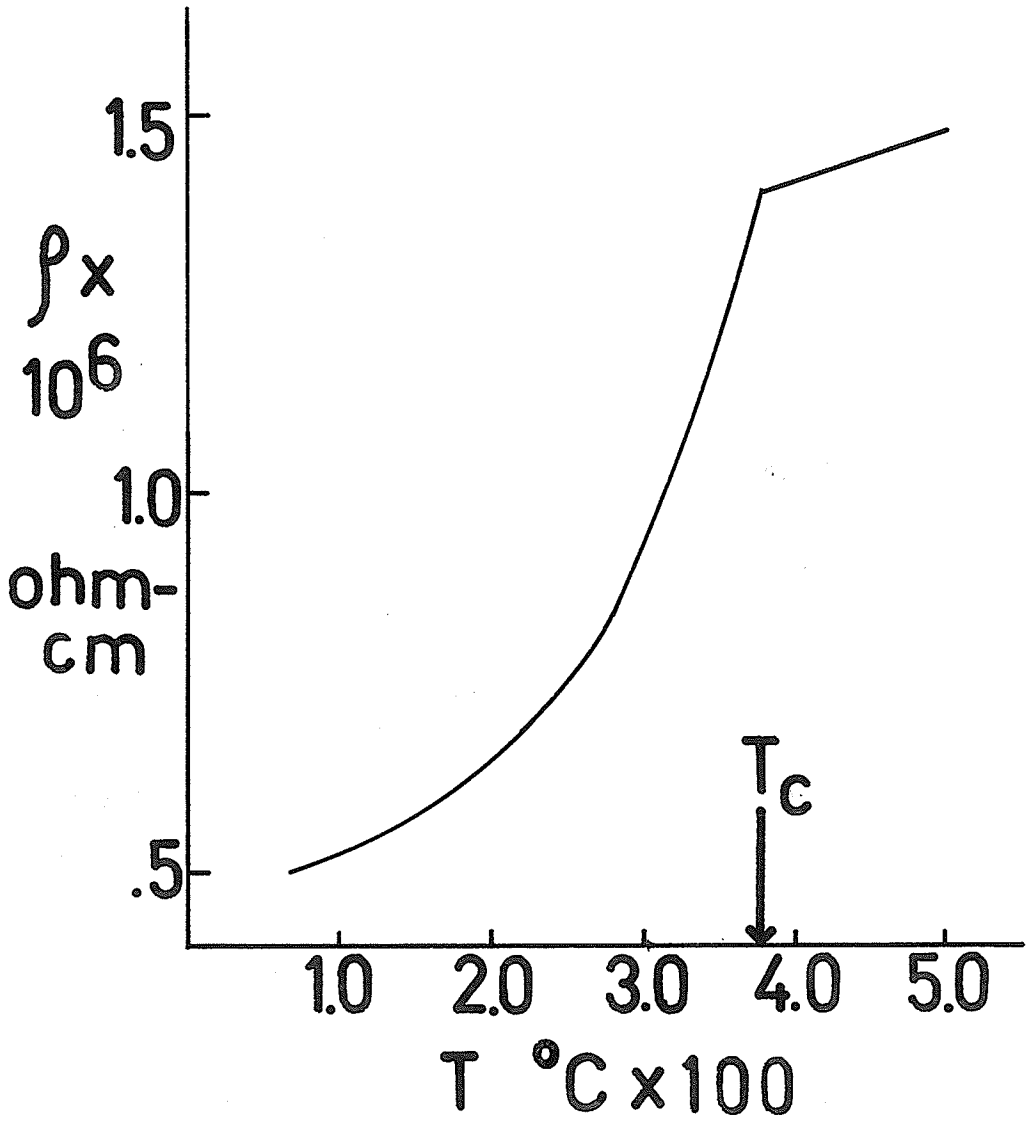

Figure 5

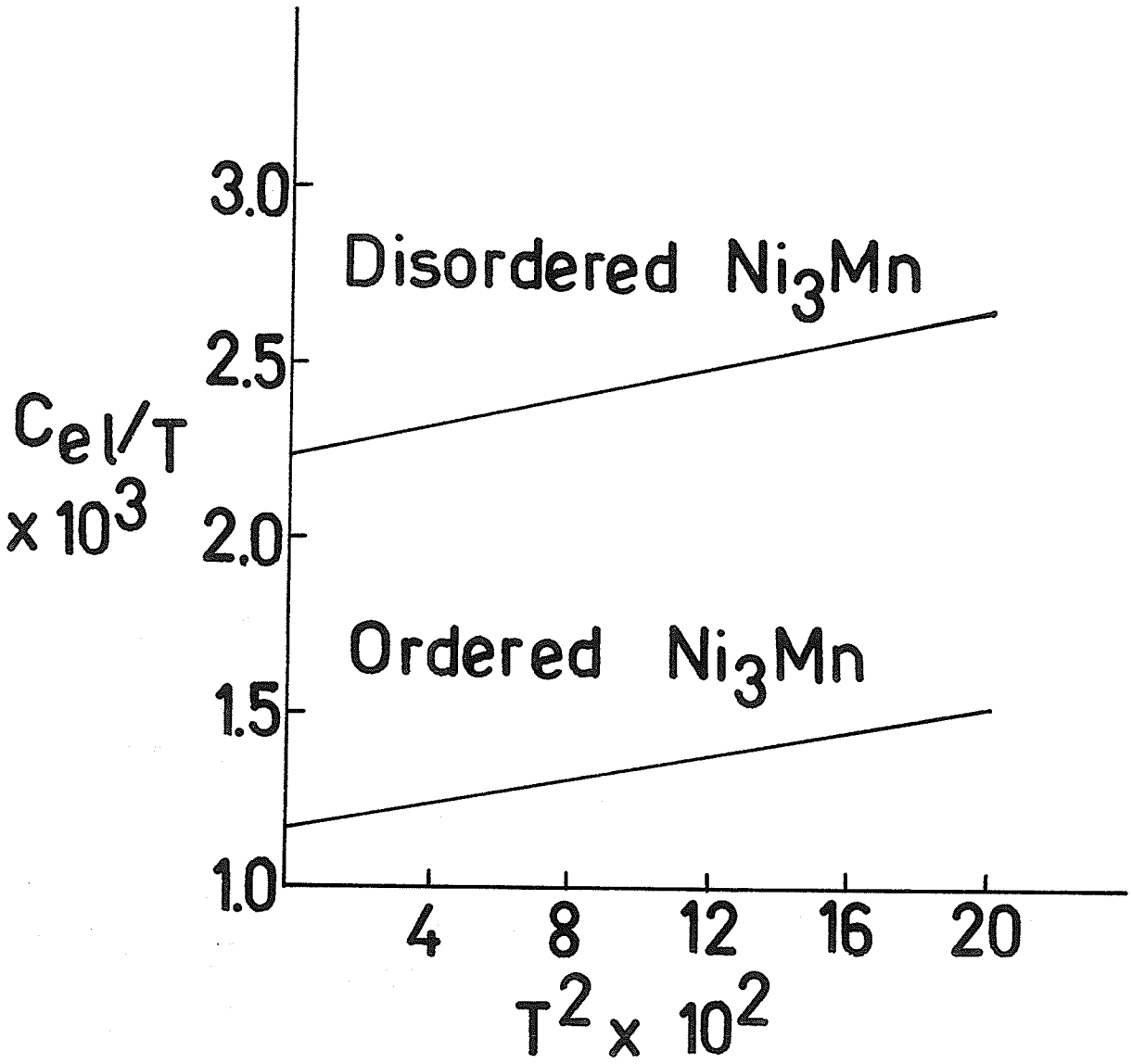
3.0
2.5
2.0
1.5
1.0
Disordered Ni_3Mn
Ordered Ni_3Mn
C_{el}/T
$\times 10^3$
4
8
12
16
20
$T^2 \times 10^2$

Figure 6

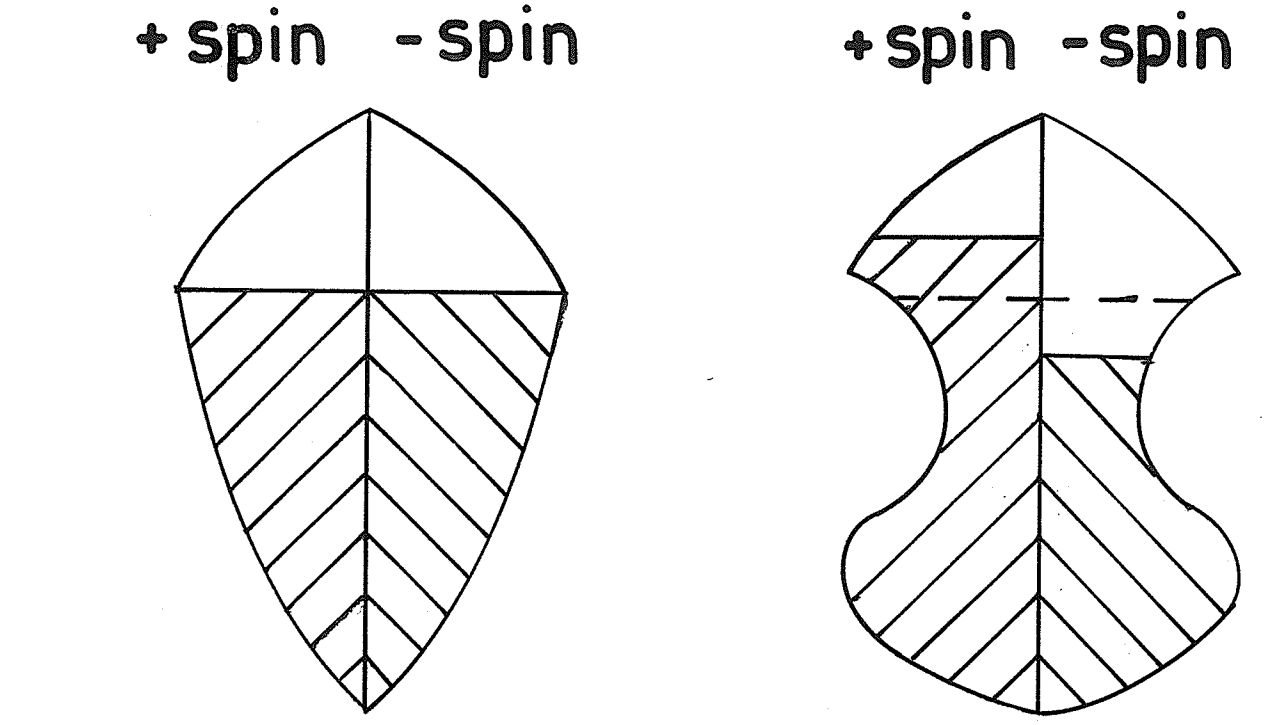

Figure 7

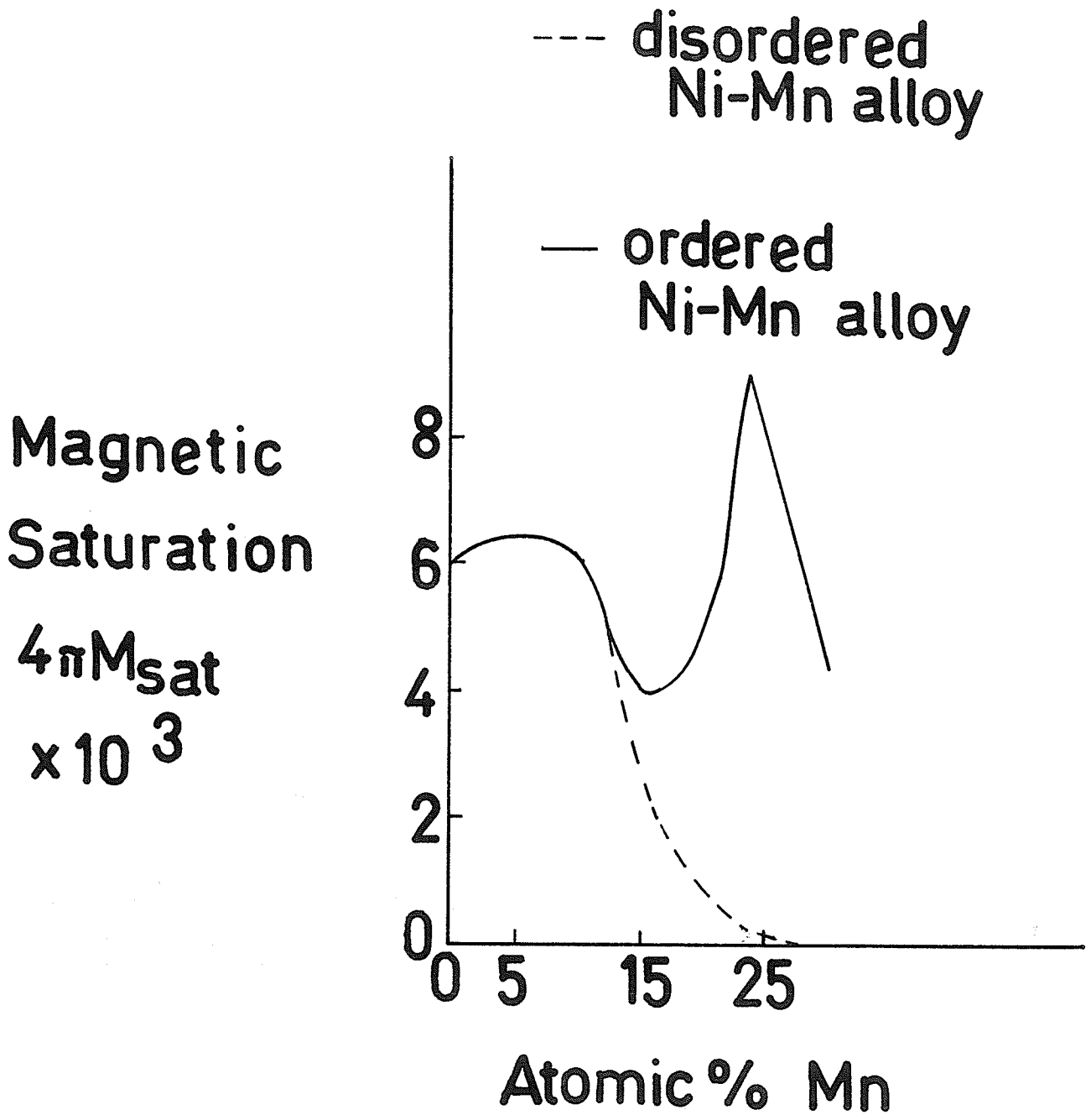
--- disordered Ni-Mn alloy
— ordered Ni-Mn alloy
Magnetic Saturation
$4\pi M_{sat}$
$\times 10^3$
8
6
4
2
0
0
5
15
25
Atomic % Mn

Figure 8

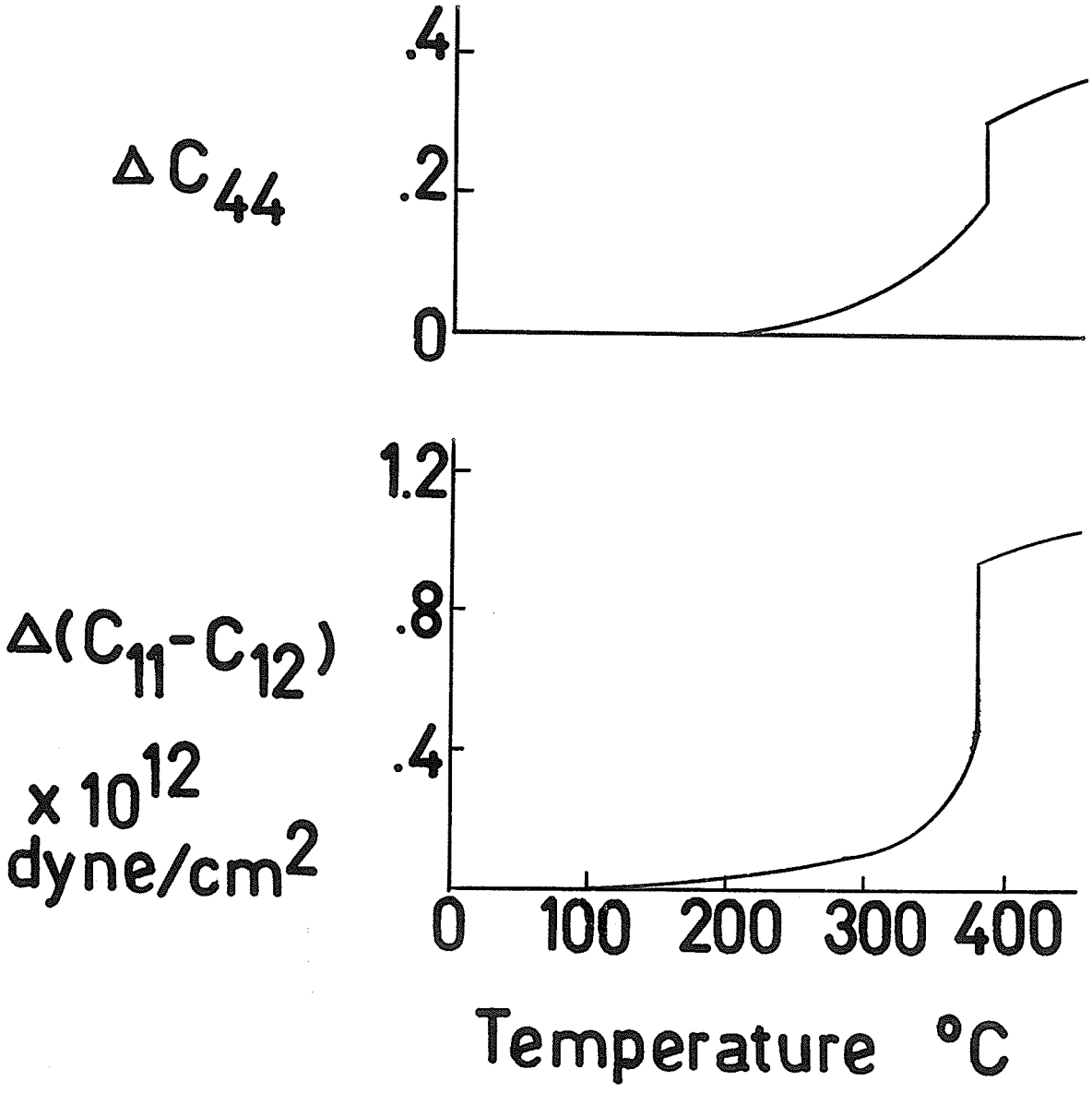
.4
.2
0
ΔC44
1.2
.8
.4
Δ(C11-C12)
x 10^12
dyne/cm^2
0
100
200
300
400
Temperature °C

Figure 9

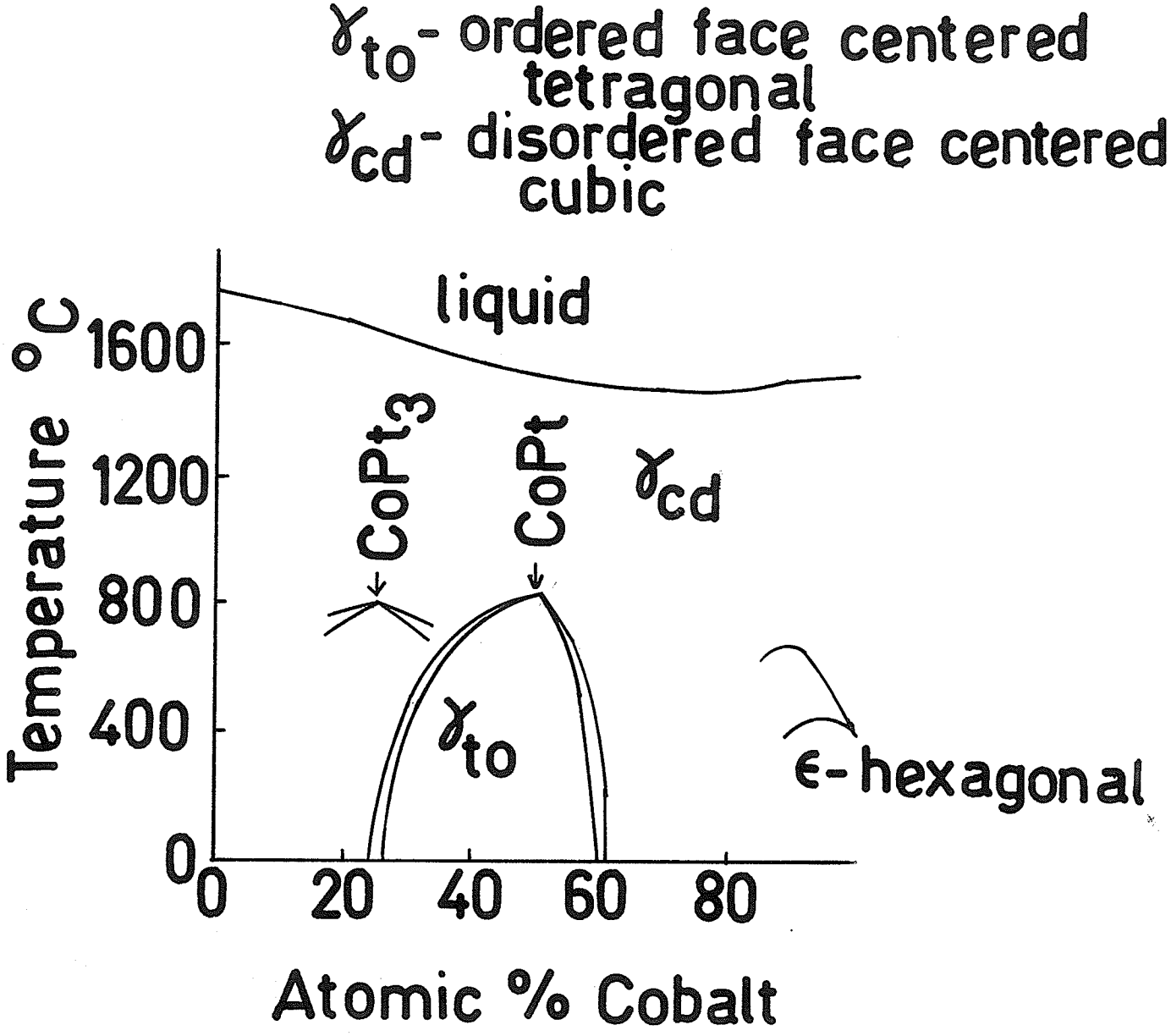
γ_{to}- ordered face centered tetragonal
γ_{cd}- disordered face centered cubic
liquid
Temperature °C
1600
1200
800
400
0
CoPt3
CoPt
γ_{cd}
γ_{to}
ϵ-hexagonal
0
20
40
60
80
Atomic % Cobalt

Figure 10

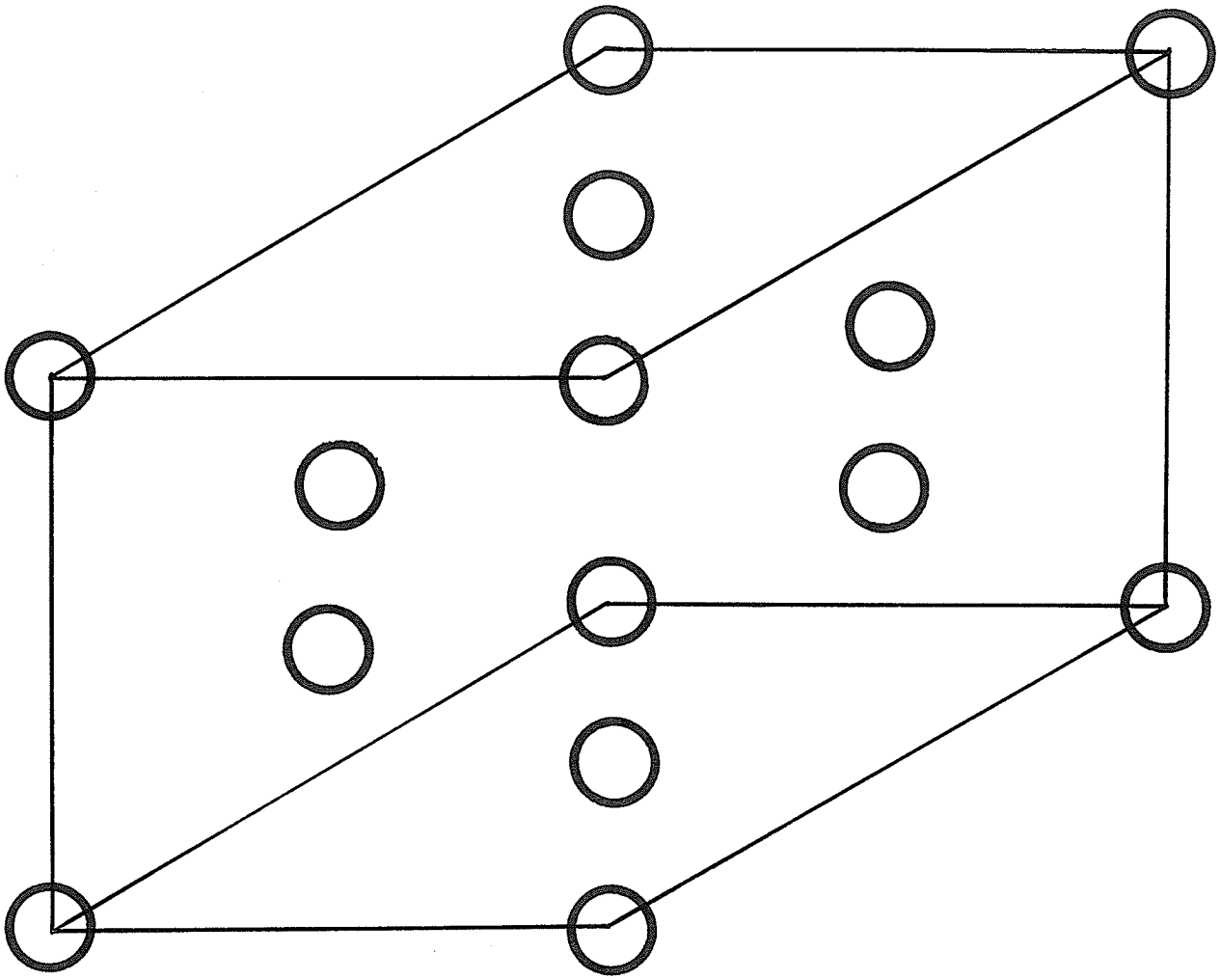

Co or Pt ○

Figure 11

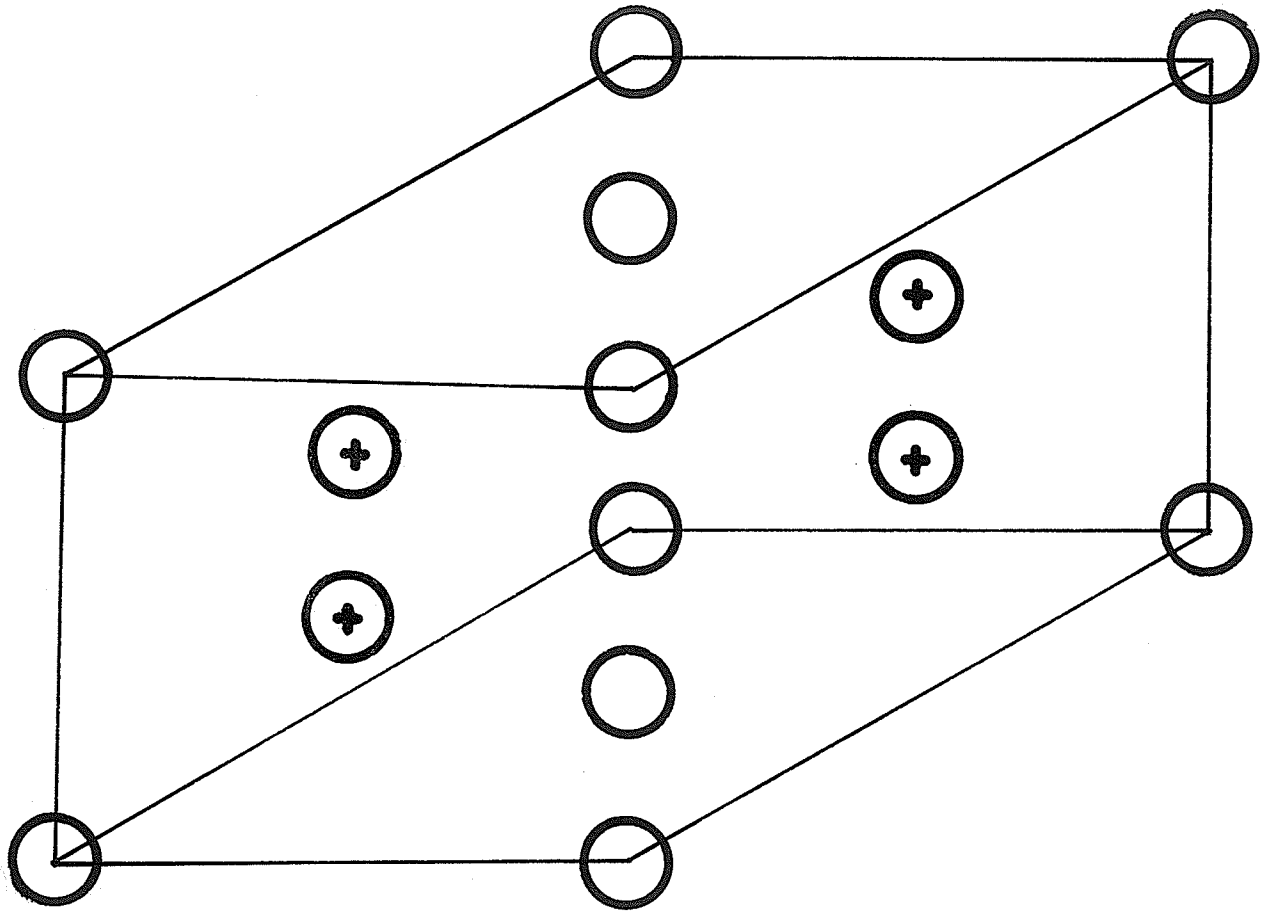

Figure 12

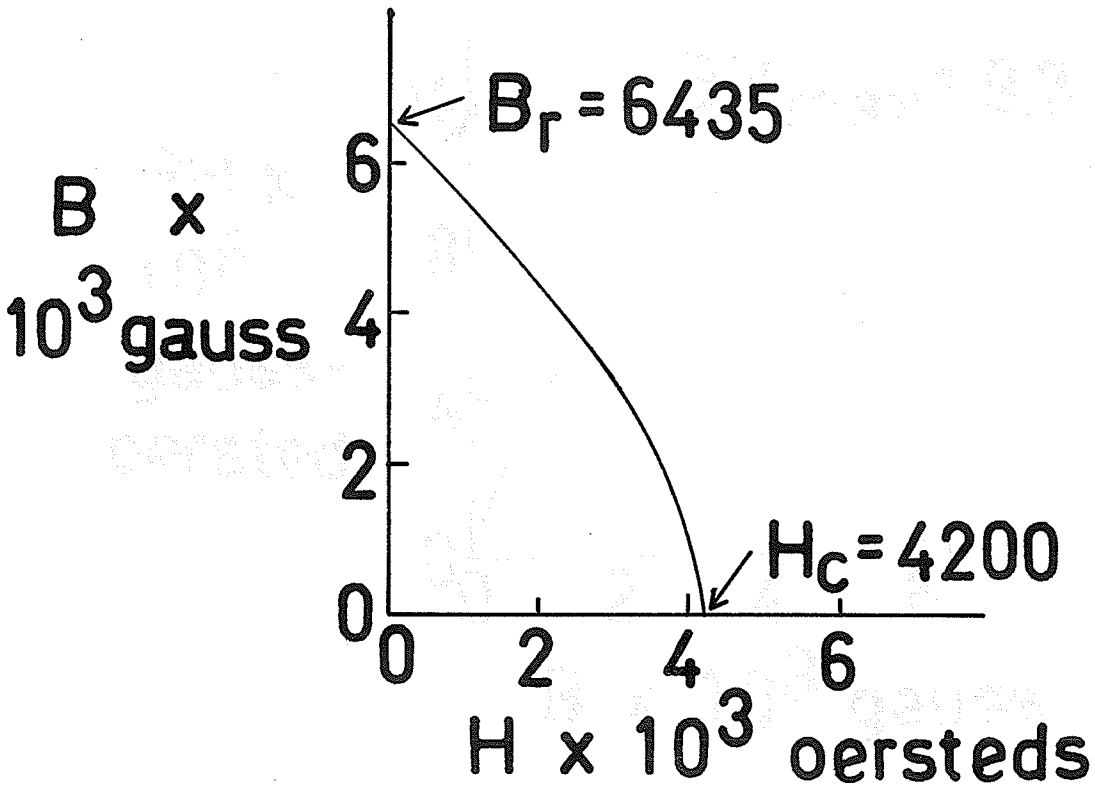

Figure 13

Table I

A atom on $\underline{a}$: $1/2(1+S)N/2$

A atom on $\underline{b}$: $1/2(1-S)N/2$

B atom on $\underline{a}$: $1/2(1-S)N/2$

B atom on $\underline{b}$: $1/2(1+S)N/2$

Table II

A atom on $\underline{a}$: $n_A(1+S)N/2$

A atom on $\underline{b}$: $n_A(1-S)N/2$

B atom on $\underline{a}$: $(n_B - n_A S)N/2$

B atom on $\underline{b}$: $(n_B + n_A S)N/2$

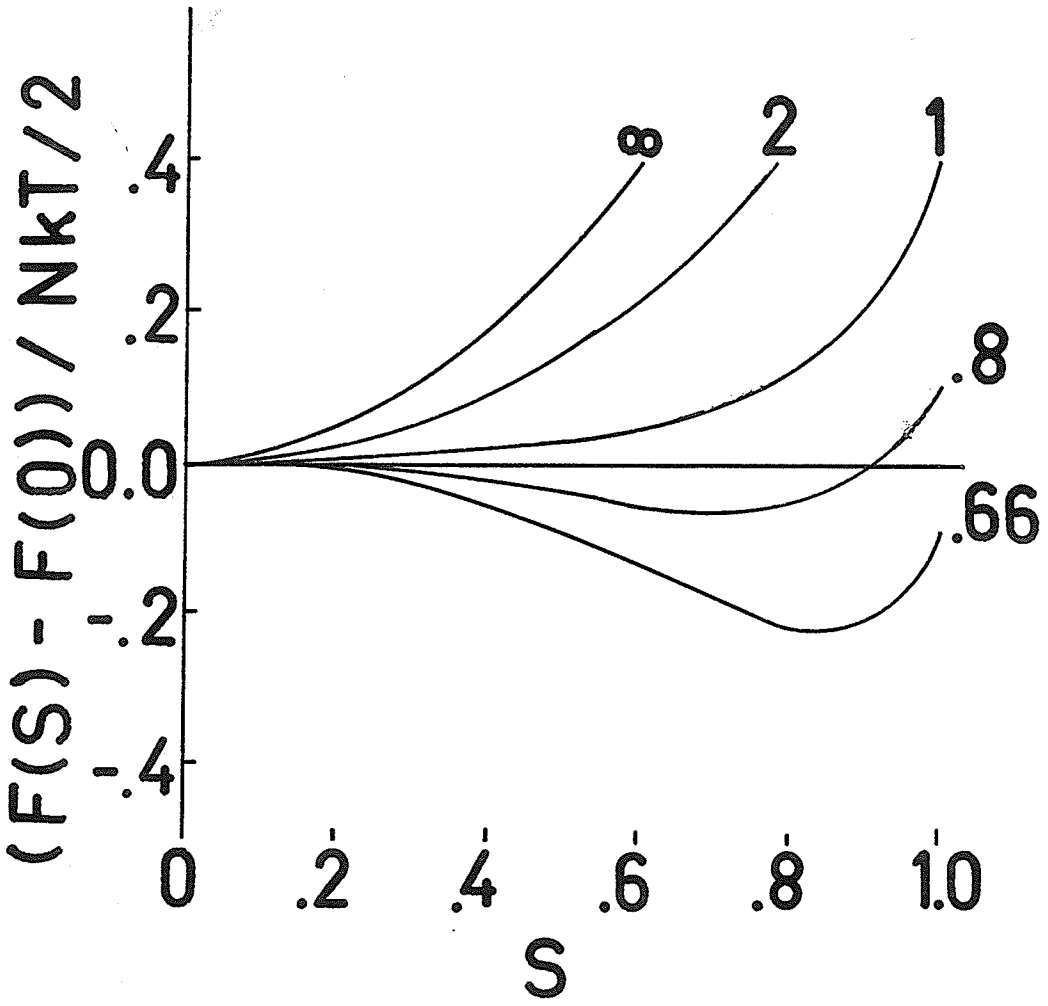

Figure 15

Table III

A on $\underline{a}$, B on $\underline{b}$: $hNf_a(1-p)/2$

A on $\underline{a}$, A on $\underline{b}$: $hNf_ap/2$

B on $\underline{a}$, A on $\underline{b}$: $hN(f_b-f_ap)/2$

B on $\underline{a}$, B on $\underline{b}$: $hN(1-2n_A+f_ap)/2$

Table IV

AA pair: $(1 - S^2)/4$

BB pair: $(1 - S^2)/4$

AB pair: $(1 + S^2)/2$

Table V

AA pair: $((1+S^2)/2)/\epsilon$

BB pair: $((1+S^2)/2)/\epsilon$

AB pair: $(1-S^2)/\epsilon$

Table VI

AA pair: $(1-S^2)/\epsilon$

BB pair: $(1-S^2)/\epsilon$

AB pair: $2(1+S^2)/\epsilon$

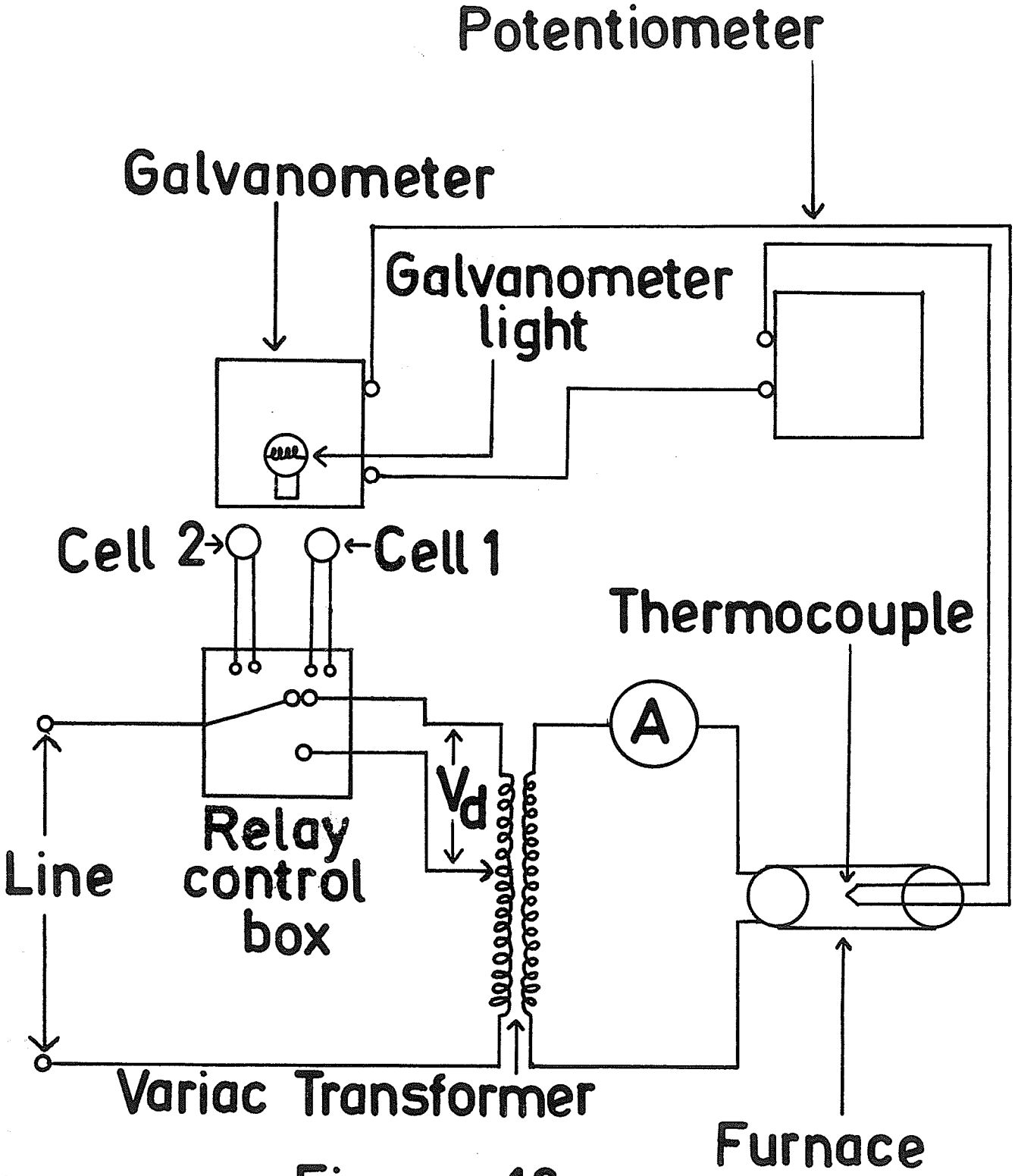
Potentiometer
Galvanometer
Galvanometer light
Cell 2
Cell 1
Thermocouple
A
Vd
Relay control box
Line
Variac Transformer
Furnace

Figure 16

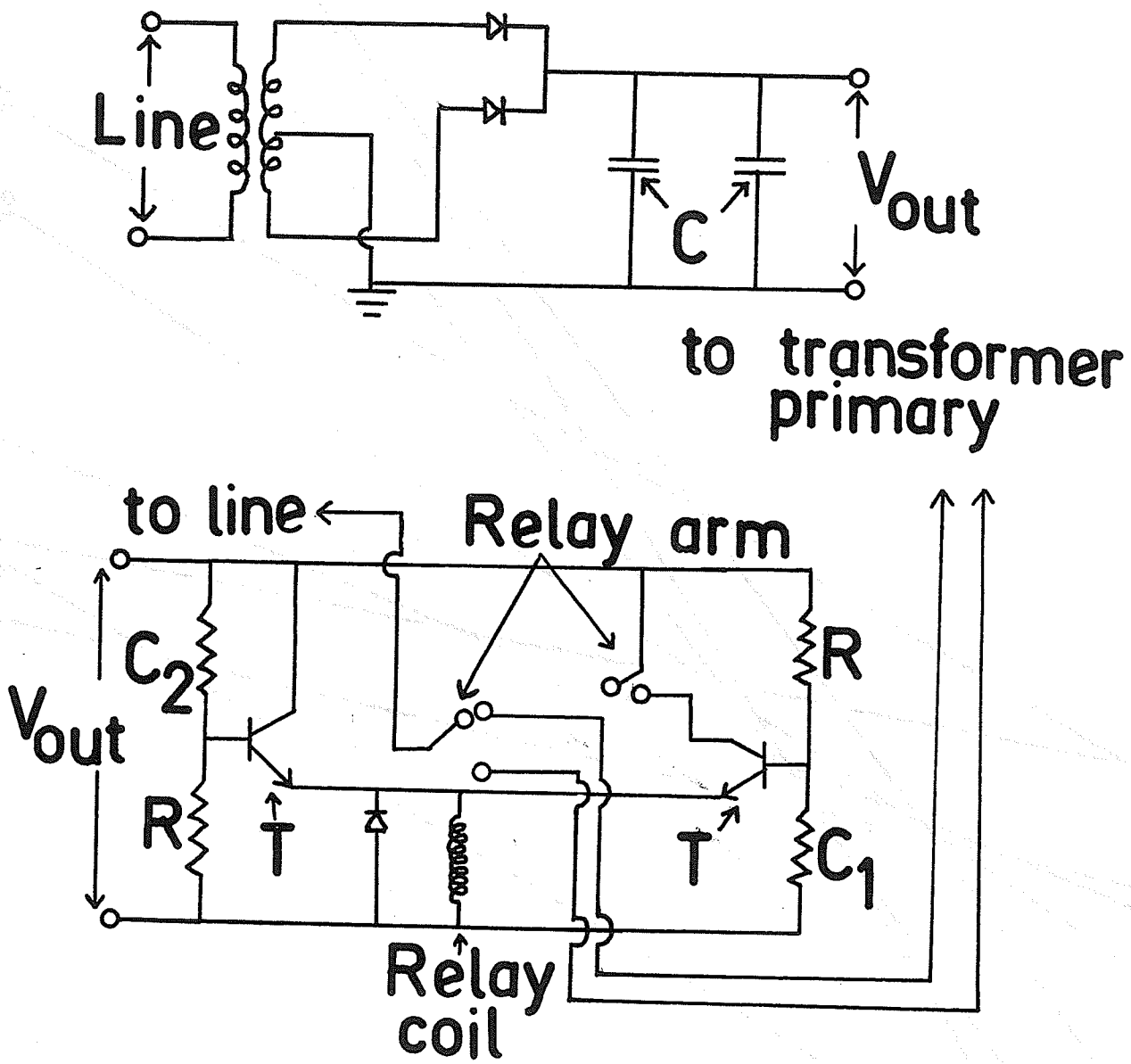
Line
C
Vout
to transformer primary
to line
Relay arm
C2
R
Vout
R
T
T
C1
Relay coil

Figure 17

TIME hours	TEMP. °C	a Å	c Å	c/a
100	620	3.801	3.685	.96948
800	700	3.799	3.695	.97227
200	750	3.797	3.699	.97414
100	775	3.797	3.701	.97456
48	800	3.796	3.701	.97497
24	805	3.795	3.702	.97544
24	808	3.796	3.704	.97567
24	810	3.795	3.704	.97592
48	812	3.798	3.705	.97544
24	815	3.795	3.703	.97583

Table VII

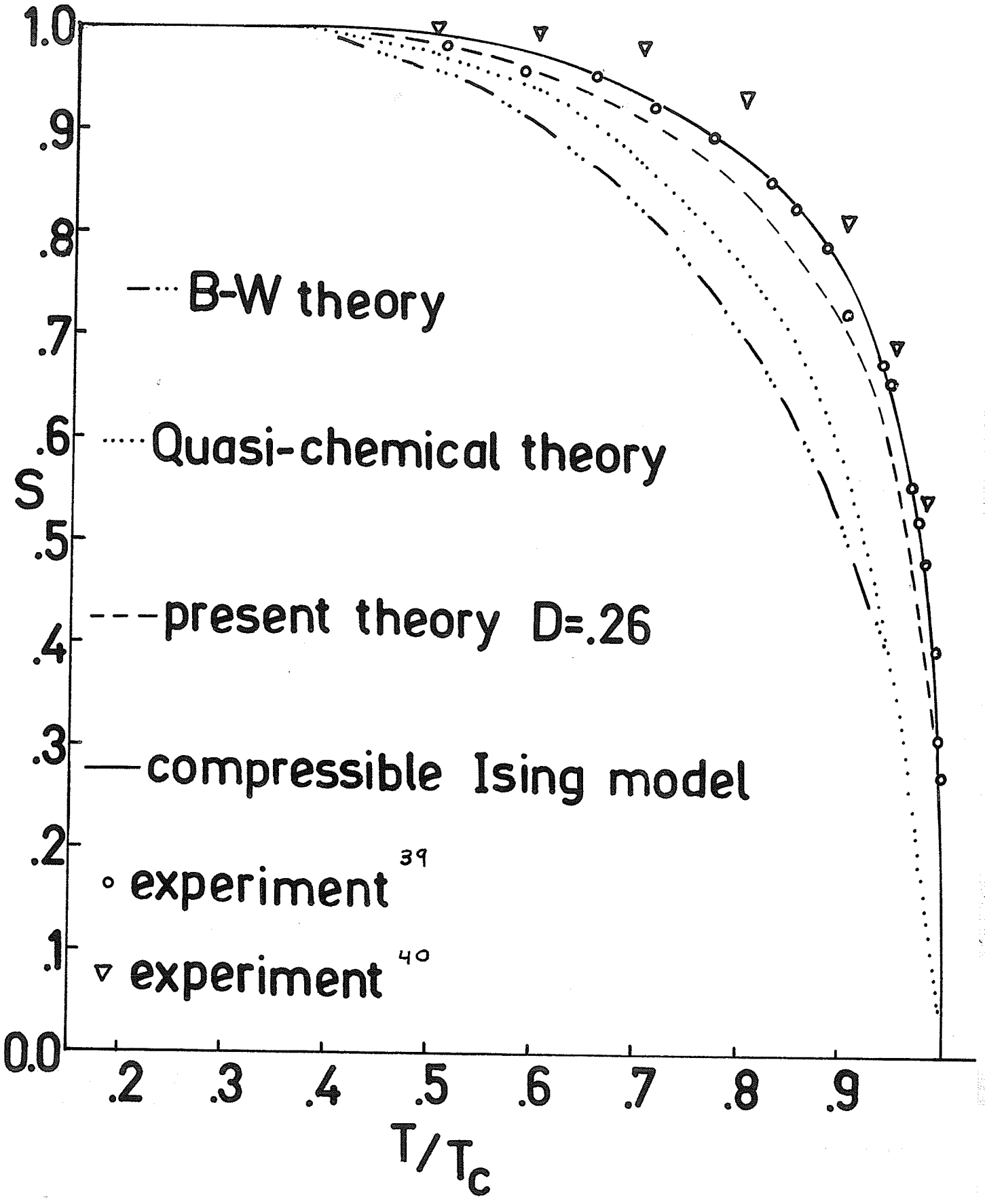
1.0
.9
.8
.7
.6
.5
.4
.3
.2
.1
0.0
S
B-W theory
Quasi-chemical theory
present theory D=.26
compressible Ising model
experiment [39]
experiment [40]
.2
.3
.4
.5
.6
.7
.8
.9
T/Tc

Figure 19

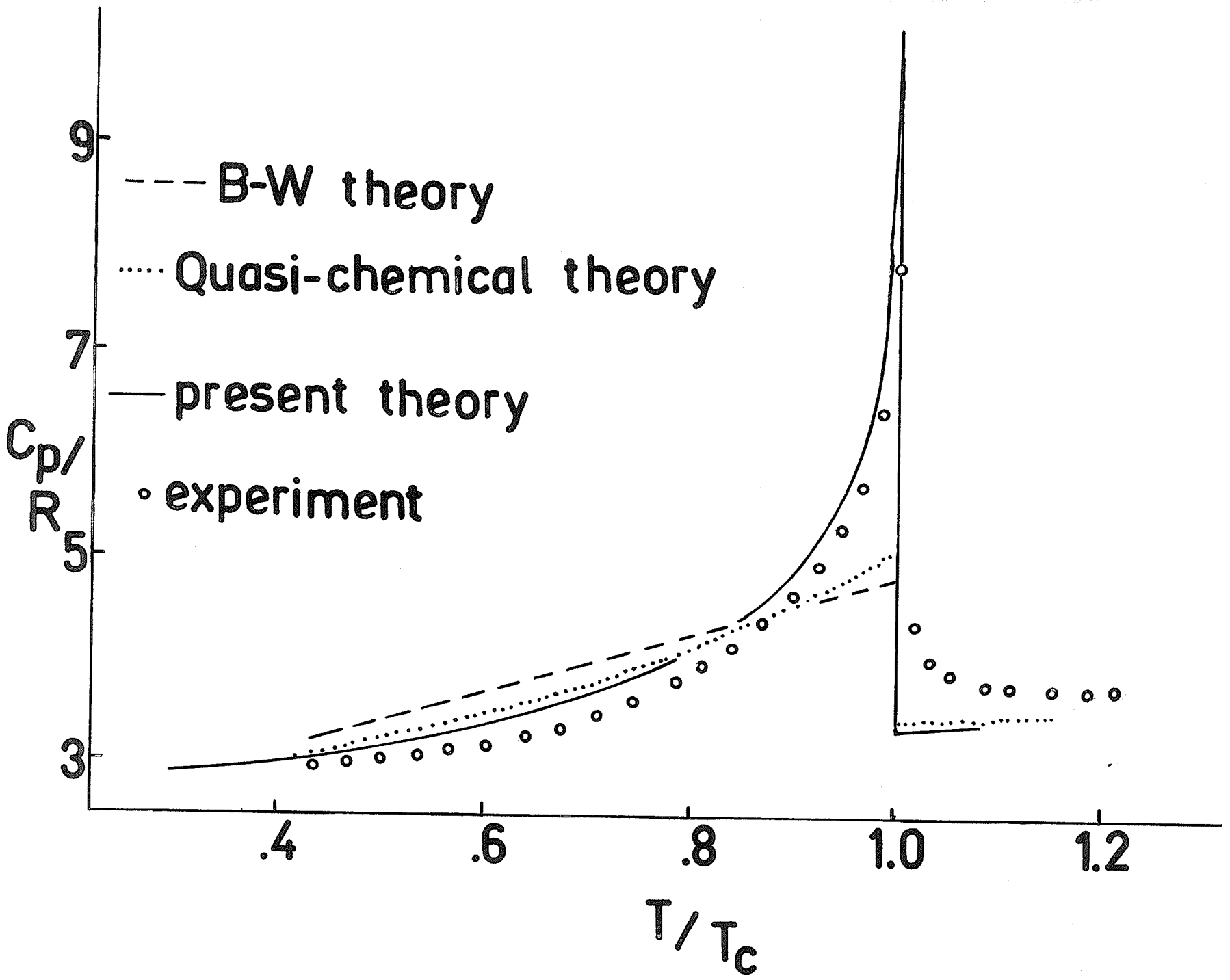
B-W theory
Quasi-chemical theory
present theory
experiment
C_p/R
9
7
5
3
.4
.6
.8
1.0
1.2
T/T_c

Figure 20

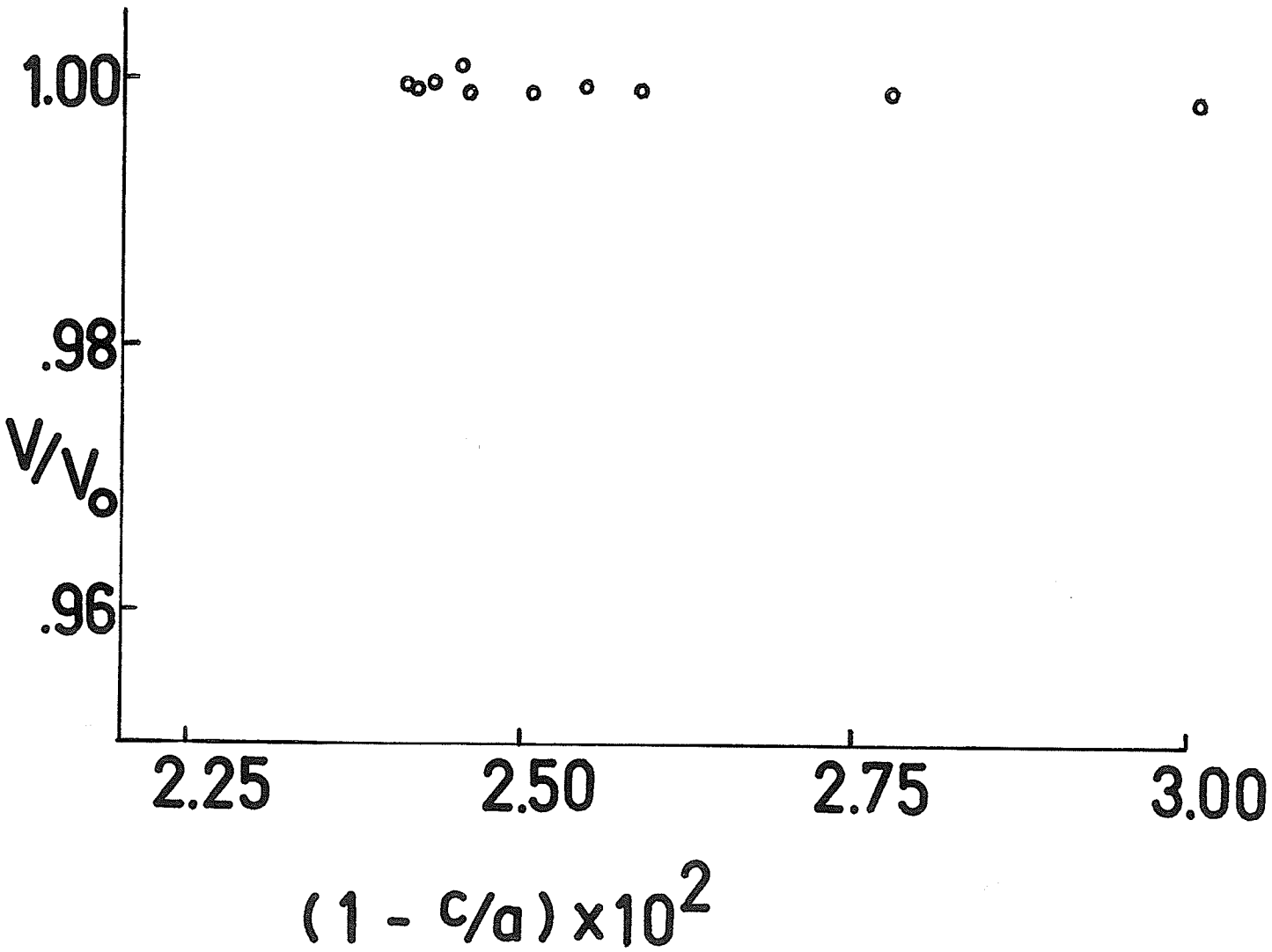

Figure 21